2005. Theoretical Population Biology (in press).

# Insect Seasonality: Circle Map Analysis of Temperature-Driven Life Cycles

James A. Powell*
Department of Mathematics and Statistics
3900 Old Main Hill
Utah State University
Logan, Utah 84322-3900
powell@math.usu.edu

Jesse A. Logan
USDA Forest Service
Rocky Mountain Research Station
Logan Forestry Sciences Lab
Logan, Utah 84321
jalogan@fs.fed.us

Submitted to *Theoretical Population Biology*

**Running Head:** *Dynamics of Insect Seasonality*

**Keywords:** *Seasonality, Developmental Timing, Circle Maps, Nonlinear Dynamics, Mountain Pine Beetle,* Dendroctonus ponderosae*, Climate Change, Global Warming*

* Corresponding author, Tel: +01 (435) 797-1953, Fax: +01 (435) 797-1822

**Abstract**

Maintaining an adaptive seasonality, with life cycle events occurring at appropriate times of year and in synchrony with cohorts and ephemeral resources, is a basic ecological requisite for many cold-blooded organisms. There are many mechanisms for synchronizing developmental milestones, such as egg laying (oviposition), egg hatching, cocoon opening, and the emergence of adults. These are often irreversible, specific to particular life stages, and include diapause, an altered physiological state which can be reversed by some synchronizing environmental cue (e.g. photoperiod). However, many successful organisms display none of these mechanisms for maintaining adaptive seasonality. In this paper we briefly review the mathematical relationship between environmental temperatures and developmental timing and discuss the consequences of viewing these models as *circle maps* from the cycle of yearly oviposition dates and temperatures to oviposition dates for subsequent generations. Of particular interest biologically are life cycles which are timed to complete in exactly one year, or univoltine cycles. Univoltinism, associated with reproductive success for many temperate species, is related to stable fixed points of the developmental circle map. Univoltine fixed points are stable and robust in broad temperature bands, but lose stability suddenly to maladaptive cycles at the edges of these bands. Adaptive seasonality may therefore break down with little warning with constantly increasing or decreasing temperature change, as in scenarios for global warming. These ideas are illustrated and explored in the context of Mountain Pine Beetle (*Dendroctonus ponderosae* Hopkins) occurring in the marginal thermal habitat of central Idaho's Rocky Mountains. Applications of these techniques have not been widely explored by the applied math community, but are likely to provide great insight into the response of biological systems to climate change.

## 1. INTRODUCTION

Maintaining an appropriate seasonality is a basic ecological requirement for all organisms. Critical life history events must be keyed to appropriate seasonal cycles in order to avoid lethal temperature or other environmental extremes, coordinate timing of reproductive cycles, avoid predation through simultaneous mass emergence and a multitude of other requirements for maintaining ecological and biological viability. Seasonality and phenology are essentially synonymous terms that have been used to describe these seasonally predictable events, although seasonality is a more general term referring to both periodic changes in the physical environment and the biological response to these changes. Phenology is specifically used to describe the seasonal progression of a series of biological stages or events. Monitoring seasonality, e.g. seasonal timing of bud-break, has recently gained additional interest as an empirical measure of global climate warming (Menzel and Fabian 1999).

Seasonal periodic cycles in photoperiod and temperature are the most obvious stimuli used to maintain an organism's internal clock, and historically the measurement of time has been closely linked to seasonal cycles (Battey 2000). Warm blooded (homeothermic) organisms expend a great deal of energy maintaining a constant thermal clock, and for homeotherms time passes at a more or less constant rate. Most organisms (all plants and cold-blooded or poikilothermic animals), however, have metabolisms varying directly with temperature. For these organisms time is relativistic; although other seasonal cues are important, life proceeds faster when things are warm, slower when things are cold. For this reason monitoring the phenology of plants and poikilotherms (particularly insects) has been used to detect empirical signals of global warming (Hill et al. 1999, Menzel and Fabian 1999).

Poikilothermic animals like insects face a balancing act when it comes to maintaining appropriate seasonality. On the one hand, it is important to maintain resiliency with respect to the vagaries of weather; e.g. to not be fooled by unusual warm spells in winter or particularly cool summers. On the other hand, it is advantageous to adapt to changing climate to exploit new environments or persist in old ones. In response to these, sometimes opposing, environmental forces, most insects have evolved physiological mechanisms, such as diapause (hibernation, or a state of arrested development that requires specific environmental cues to be terminated) and sensitivity to photoperiod, which serve to re-set and maintain the seasonal clock. Although diapause is an expected norm, many insects, even those living in temperate environments with strong seasonality, apparently lack diapause or any other physiological timing mechanisms. These insects have seasonality that is under direct temperature control (Danks 1987). Insects with direct temperature control are of particular interest with respect to global change because their phenology should respond immediately, and predictably, to a warming climate.

For insects with direct temperature control of seasonality how can an appropriate seasonality be maintained without some physiological timing mechanism? Adaptive seasonality occurs when 1) individuals emerge at the same time (synchrony), 2) individuals emerge at an appropriate time to utilize resources (timing), and 3) life cycle events are paced to avoid lethal extremes of temperature and environment (seasonality). Gurney et al. (1992) demonstrated that development-free diapause in some life stage is sufficient to cause phase-locking with the seasonal temperature cycle in a theoretical two-stage organism, and expanded on their results in a series of other papers regarding two-stage organisms (Gurney et al. 1994; Grist and Gurney 1995). Our past work (Bentz et al. 1991, Logan and Bentz 1999, Powell et al. 2000) has explored adaptive seasonality for the mountain pine beetle, *Dendroctonous ponderose* Hopkins.

The mountain pine beetle is of considerable ecological and economic interest. This insect, which spends its entire developmental life under the bark of host pine trees, is an aggressive tree killer (Samman and Logan 2000). For this reason, there has been an extensive history of field collection and laboratory rearing for this species. This extensive experience, in our laboratory and others, has failed to indicate diapause or any other physiological timing mechanism other than temperature. Winter collected, or chilled individuals, resume development immediately on warming (Wygant 1942, Logan and Amman 1986). Individuals collected from the field in summer can be reared through to adult without chilling (Reid 1962, Safranyik and Whitney 1985). No differences in developmental rates are observed between individuals held in cold storage from those reared directly from field collections (J.A.L., unpublished data and personal observations). Considering these observations, and no counter-evidence that we are aware of, it is reasonable to assume that phenology and seasonality are under direct temperature control for the mountain pine beetle.

Although no evidence exists for diapause the mountain pine beetle exhibits developmental quiescence when temperatures fall below developmental thresholds. Quiescence, in contrast to diapause, occurs when temperatures are so extreme that no development occurs, as when winter temperatures reach such lows that the physiology of the organisms essentially stops for developmental purposes. Unlike diapause, quiescence is reversed as soon as temperatures leave the extreme range; for mountain pine beetle both quiescence and development occur on almost every winter day in the year as temperatures drop below a thermal threshold at night and then rise above with solar heating during the day. The requirement for synchronous adult emergence for mountain pine beetle is fully described in Logan and Powell (2001), but briefly, a spatio-temporal distribution of oviposition dates must be focused onto a temporally

synchronous adult emergence curve to provide the large numbers of attacking beetles required to overcome the substantial defenses of host trees (Raffa and Berryman 1987). The analytical tools we have developed to analyze phenology and predict seasonality in the mountain pine beetle provide a general framework for any plant or animal with phenology under direct temperature control. Even for organisms with other timing mechanisms (e.g. diapause) or secondary emergence cues (e.g. photoperiod) methods described here can easily be adapted, as we will point out below.

In this article we explore the quantitative modeling and analysis of direct temperature control and how these models shed light on adaptive seasonality. We first set the mathematical framework for modeling seasonality under the direct influence of temperature; next, we describe analytical tools that result from this framework; and finally, we describe two examples from our work with mountain pine beetle. These examples illustrate the application of seasonality theory to predict the consequences of global warming on an important disturbance agent in North American conifer forests. Insects are potentially good indicator species because of their economic importance, which has resulted in a large database for model parameterization (Logan et al. 2003). The analytical framework described here is generally useful for predicting consequences of warming climate on a species-specific basis. Such predictions can identify climatically responsive indicator variables, predict ecological consequences of global warming, and provide strong inference regarding invasion potential by exotic species.

## 2. MODELING AND PREDICTING DEVELOPMENTAL MILESTONES

### 2.1. Temperature Dependent Models

Relating temperature to the development of insects requires differentiating between *age* and *stage*. Although both are related to time, age is chronological in nature and may not be

directly observable; stage is a developmental concept typically defined by distinct morphological characteristics often requiring a molt for transition from one stage to the next. *Developmental rate* is the speed of progression through an instar, or stage, and is dependent on temperature in a predictable fashion. Assuming that it is the same function throughout a stage, the developmental rate, $r(T)$, at a constant temperature, $T$, is the inverse ($1/t$) of the time required to complete that life stage. The developmental index, $a_j$, or age in stage $j$, is then the fraction of the $j$th life stage completed at any particular time by the median individual in the population, and is not directly observable. It is related to the developmental rate by a differential equation

$$\frac{d}{dt}a_j(t) = r\left[T(t)\right];\;\; a_j(t = t_{j-1}) = 0;\;\; a_j(t) = \int_{t_{j-1}}^{t} r_j\left[T(t)\right]dt;\;\; a_j(t = t_j) = 1. \qquad [1]$$

What is observable are developmental milestones, or transition times between life stages.

Life stage $j$ begins at time $t_{j\text{-}1}$, which is the time of completion of the previous life stage ($t_{j\text{-}1}$, as indicated by the initial condition of the differential equation above), and finishes at that time, $t_j$, when $a_j = 1$. Numerically, *developmental increments*, $\Delta a_j = r[T(t)]\Delta t$, during short time steps, $\Delta t$, are summed over time until $a_j = 1$, which indicates completion of life stage $j$ and defines $t_j$, the time at which life stage $j$ terminates and $j+1$ is initiated.

These relationships underlie almost all models of insect phenology (see Logan & Powell 2001). Once the mathematical relationship between temperature (or other environmental variables), time, and physiological age is defined, there remains the issue of finding an appropriate functional relationship between temperature, $T$, and the developmental rate, $r(T)$.

**2.2. Developmental Rate Functions**

The earliest functional form used to describe the relationship between temperature and rate of development was the linear or *day-degree* model, a concept that dates to the 1700s (Wang

1960), and has been extensively used to model both animal and plant phenology. These models assume that temperature (in degrees) and development (in days) relate linearly, so that a developmental event is timed by accumulation of a certain number of hours of total temperature above some arbitrary threshold. Day-degree models often work well if the temperatures of ecological interest do not fall outside of the linear region of the organism's thermal response. Their advantage is simplicity; their disadvantage is that they only constitute a more or less adequate approximation (Wang 1960).

The observation that developmental rates are nonlinear was made over 60 years ago (Janisch 1932). It was not until the mid 1970s that the use of nonlinear rate functions became widely practiced, mostly in response to the widespread availability of digital computers, which provided methods for parameter estimation and convenient numerical solution of equation [1]. Stinner et al. (1975), Logan et al. (1976), and Sharpe & DeMichele (1977) described nonlinear functions for insect temperature dependent developmental rates that have been widely applied since their introduction. This large body of literature indicates that developmental rates have an exponential phase at low temperatures, increase to an optimum, and then decline sharply from the optimum temperature to a lethal thermal maximum. Parameter estimation for nonlinear developmental rate models is more complex than for linear based day-degree models. Estimation procedures for non-linear rate functions have been automated for a reasonable suite of equations (Wagner et al. 1984, Logan 1988). A nonlinear rate model is required whenever simulations must cover temperatures over the full range of physiological activity.

Life cycle phenomena involving temperature extremes (diapause for example) also require nonlinear representation. Some timing mechanisms, sensitivity to photoperiod or availability of resources for foraging, may require higher dimensional models for progress

through a stage. In all cases, the influence of environmental factors on rate of progress through a life stage needs to be modeled. It is not our goal here to review all possible models of phenology, but rather to provide a framework for evaluating their dynamic consequences for adaptive seasonality. We will illustrate the methodology under the assumption of direct temperature control, but extension to more complex methods of timing is possible provided that output developmental milestones depend deterministically on the time of termination of the previous life stage and parametrically on environmental factors, as described below.

**2.3. Determining Ovipositional Dates from Year to Year**

When developmental rate curves are determined for all stages of an insect's life cycle, the question becomes how should they be used to make predictions regarding adaptive seasonality? Returning to equation [1] and direct temperature control, solutions can be written by integration,

$$a_j(t) = \int_{t_{j-1}}^{t} r_j\big(T(s)\big)\,ds.$$

Unlike traditional differential equations, where the aim is to investigate the structure of the solution, in this case we wish to determine when the solution reaches $a_j=1$, corresponding to the termination of the $j$th life phase. This time, $t_j$, is defined implicitly using the solution to the differential equation [1] and the condition $a_j(t_j) = 1$,

$$1 = a_j(t_j) = \int_{t_{j-1}}^{t_j} r_j\big(T(s)\big)\,ds.$$

It is generally impossible to evaluate this integral analytically and even less possible to find an explicit expression for $t_j$, and we resort to numerical solution. The time at which the numerical integral exceeds one is the computational approximation to $t_j$.

Given a sufficiently long series of temperature measurements and a set of rate curves for all $N$ stages of an organism, we have outlined a mathematical approach to calculating the

sequence of times of developmental milestones, $t_0, t_1, t_2, \ldots, t_N,$ corresponding to the date of oviposition ($t_0$), hatching of the eggs ($t_1$), progression through larval instars and whatever other stages of life history occur, culminating in the emergence of the reproductive adult and oviposition ($t_N$). The reproductive input from adults of one generation is the initial condition for the egg stage of development in the next generation; we therefore introduce the notation $t_0^n$ to indicate the median date of oviposition in the *n*th generation, and connect with the sequence of dates of developmental milestones

$$t_0^n = t_0, t_1, t_2, \ldots., t_{N-1}, t_N = t_0^{n+1}.$$

This sequencing mathematically captures the essential circularity of life history, in which egg begats egg through the intermediaries of adults and the other developmental phases.

## 3. CIRCLE MAPS, THE *G* FUNCTION, AND PHENOLOGICAL DYNAMICS

### 3.1. Defining the *G* Function Circle Map

There is additional circularity inherent in the progression of seasons and the rotation of Julian dates from 0 to 365 and back again. Temperatures are also, in broad strokes, periodic functions of the time of year. We assume periodicity, and discuss later how deviations alter results. If we assume periodicity in temperatures from year to year, and interpret the sequence of ovipositional dates modulo 365 according to the Julian calendar, we have constructed a mathematical circle map. By this we mean that, for a given periodic temperature signal, the output oviposition date, $t_0^{n+1}$, depends directly and uniquely on the oviposition date for the previous generation,

$$t_0^{n+1} = G\left(t_0^n\right),$$

where $t_0^n$ and $t_0^{n+1}$ are Julian dates (not interpreted modulo 365). This function mapping generation to generation, or `*G* – function' will be the basis for the mathematical analysis of

phenology and seasonality. It generates a circle-map if both $t_0^n$ and $t_0^{n+1}$ **are** interpreted modulo 365, that is, with respect only to *time* of year, but not year.

When the *G* function has a fixed point, that is, if there is a day in the year, $t^*$, for which

$$t^* + 365 = G(t^*),$$

then the population has a fixed number of generations per year. When this fixed point is stable (that is, when nearby oviposition dates converge to the fixed point as the map is iterated from year to year) the entire population will synchronize on an oviposition date at the fixed point, thus satisfying two of the three requirements for an adaptive seasonality. The third requisite, appropriate timing, can be evaluated by determining if a stable, univoltine fixed point falls within a window of allowable dates which depends on individual species life history.

In what follows we will discuss one and two life stage examples, then turn our attention to a general understanding of circle maps representing multi-stage phenologies. This theory will then be applied in the context of the Mountain Pine Beetle (*Dendroctonus ponderosae* Hopkins), an important forest insect capable of spectacular outbreaks in univoltine temperature regimes.

**3.2. Single-Stage Models**

The simplest possible phenology model would be a single stage model, with only one rate curve, $r_1(T)$, and a given, periodic temperature record. The well-known degree-day models are an example of this kind of model if *r* is linear. We define

$$R_1(t) = \int_0^t r_1(T(s))\, ds$$

to be the cumulative developmental index; the condition relating oviposition dates in two subsequent generations is

$$R\left(t_0^{n+1}\right) - R\left(t_0^{n}\right) = \int_{t_o^n}^{t_0^{n+1}} r_1\left(T(s)\right) ds = 1.$$

Suppose that a univoltine fixed point exists, that is, a $t^*$ with

$$1 = R\left(t^* + 365\right) - R\left(t^*\right).$$

Then

$$1 = \int_{t^*}^{t^{*1}+365} r_1\left(T(s)\right) ds = \int_{0}^{365} r_1\left(T(s)\right) ds,$$

because $T$ is periodic over the year. Thus *every* day of the year generates a separate, univoltine fixed point, since the developmental index integrates to one starting at any point in the year.

Clearly in this case synchony is lost, since no fixed point can move closer to or further from any other. In addition these univoltine solutions for one stage models are not structurally stable, that is, univoltinism will not be preserved if rate curves or temperatures are perturbed. To illustrate, suppose development is constant above some threshold,

$$r_1 = \begin{cases} \rho_1, & T \geq \theta_1, \\ 0, & T < \theta_1, \end{cases}$$

and let temperatures be sinusoidal, modeling the seasonal temperature swing:

$$T = T_0 - T_1 \cos\left(\frac{2\pi}{365} t\right).$$

Here $t=0$ on New Year's Eve, loosely the coldest time of the year, and for simplicity we will assume temperatures don't drop below threshold. A univoltine solution exists if

$$R_1(365) = \int_0^{365} \rho_1\left(T_0 - T_1 \cos\left(\frac{2\pi}{365}t\right)\right) dt$$
$$= \rho_1\left[365\,T_0 - \frac{365}{2\pi}\sin\left(\frac{2\pi}{365}t\right)\Big|_{t=0}^{t=365}\right]$$
$$= \rho_1 365\,T_0 \overset{must}{=} 1.$$

So, univoltine solutions require the developmental rate to precisely equal the inverse of the number of degree-days in the year. A similar result holds for nonlinear rate curves and more complicated temperature records. Consequently, if temperatures are changed in the slightest way this condition will be violated and univoltine solutions will not exist. The more general circumstance for one stage models is that the sequence of oviposition dates will rotate around the year and never repeat, a situation clearly at odds with maintaining seasonality. One-stage models are therefore incapable of reflecting adaptive seasonality.

**3.3. Two Stage Models**

The situation is quite different for two or more life stages. Consider an organism with two developmental stages, one in which development proceeds linearly with temperature above a given threshold and a second in which development is constant with temperature above a different threshold. Rate curves would be given by

$$r_1 = \begin{cases} \rho_1(T - \theta_1), & T \geq \theta_1, \\ 0, & T < \theta_1, \end{cases} \qquad r_2 = \begin{cases} \rho_2, & T \geq \theta_2, \\ 0, & T < \theta_2. \end{cases}$$

Given a starting oviposition date, $t_0$, and taking the simple periodic yearly temperature model above, the date of egg hatching for the median individual, $t_1$, can be calculated

$$1 = \int_{t_0}^{t_1} \rho_1\left[T_0 - T_1 \cos\left(\frac{2\pi}{365}t\right) - \theta_1\right] dt = \rho_1\left[(T_0 - \theta_1)(t_1 - t_0) - T_1 \frac{365}{2\pi}\left(\sin\left(\frac{2\pi}{365}t_1\right) - \sin\left(\frac{2\pi}{365}t_0\right)\right)\right].$$

The second life stage starts at time $t_1$ and the time at which it terminates, $t_2$, satisfies

$$1 = \int_{t_1}^{t_2} \rho_2 \, dt = \rho_2 (t_2 - t_1).$$

The end of the second life stage begins with oviposition of the next generation, as discussed above. For a univoltine solution to exist, the date of termination of the second life stage must equal the original oviposition date plus 365, and we define $t^* = t_0 = t_2 - 365$ to be such a univoltine solution, if it exists. The two relations can be graphed on the same axes using the following graphical trick, illustrated in Figure 1. Each curve may be graphed separately and modulo 365, and in the second curve the identification of $t_2$ with $t_0$ amounts to reflection of the graph about the line $t_2 = t_1$. Combining the graphs as in Figure 1(c), univoltine solutions emerge as locations where the two curves cross.

The combined phenology graph can be used to illustrate the dynamic properties of the two stage phenology model and of univoltine fixed points. Graphically, iterating the circle map through two life stages amounts to `cobwebbing' between the curves representing output of the first life stage and reflected output of the second life stage, as illustrated in Figure 2. Iterates bounce horizontally from the first life stage curve to the second, then vertically from the second to the first. One of the two univoltine solutions is unstable and repels sequences of oviposition dates, which converge to the second, stable univoltine solution, which we will label $t^*$.

While these two curves are the output of very simple and specific temperature and rate curves, the concepts illustrated are quite general. Two phenology curves, one reflected and graphed on the same axes as the first, may or may not cross. However, if they *do* cross a stable-unstable pair of univoltine fixed points will be created. These fixed points are structurally stable; altering either the rate curves or the temperatures slightly may move the exact location of the curves, but will not change the fact that they intersect. Thus, stable-unstable univoltine fixed points can be expected to exist for a broad range of parameters (an open set, mathematically),

both in terms of the rate curves and the temperature record. In particular, sufficiently small interannual variability in temperatures will not alter univoltinism significantly.

Generally speaking, this is the picture for two or more life stages – structurally stable univoltine fixed points in broad parameter regimes. The only difficulty is that the dynamic mapping illustrated above is just a two-dimensional trick; for three or more life stages the technique is too cumbersome to be useful. The *G* function, a mapping directly from oviposition dates in one generation to oviposition dates in the next, will allow us to extend the dynamic analysis to multiple life stages.

### 3.4. Definition of the *G* Function for *N* Life Stages

Consider the development of a multi-stage organism. For each of *N* life stages there is a rate curve, $r_j(T)$, and an associated cumulative developmental index,

$$R_j(t) = \int_0^t r_j\big(T(s)\big)\,ds.$$

The relationship between the time of inception, $t_{j-1}$, and the time of termination, $t_j$, of the *j*th life stage is given by

$$1 = \int_{t_{j-1}}^{t_j} r_j\big(T(s)\big)\,ds = R_j(t_j) - R_j(t_{j-1}).$$

This determines $t_j$ uniquely in terms of $t_{j-1}$, and therefore the end of the final life stage, $t_N$, is uniquely determined in terms of the starting oviposition date, $t_0$. Since the termination of the final, adult life stage can be viewed as oviposition in the next generation, this allows us to write

$$t_0^{n+1} = G\big(t_0^n\big),$$

where $t_0^n$ is the date of oviposition in the *n*th generation. In general the *G* function can not be written down analytically, but it can be calculated numerically by:

1. For each life stage, *j,* calculate the cumulative developmental index, $R_j(t)$, for the given temperature series (which must be expanded into a two year series).

2. For each oviposition date, $t_0$, between 0 and 364:
    a. Find $t_1$ for this oviposition date by searching for the first value of $t$ which gives $R_1(t) = R_1(t_0) + 1$.
    b. Find $t_2$ for the previous $t_1$ by searching for the first value of $t$ which gives $R_2(t) = R_2(t_1) + 1$.
    c. Repeat …
    d. Find $t_N$ for the previous $t_{N-1}$ by searching for the first value of $t$ which gives $R_N(t) = R_N(t_{N-1}) + 1$.
    e. Save $t_N$ as the numerically calculated value of $G$ for this value of $t_0$.

(See Table 1 for a glossary of parameters, variables and functions.) This simple computational algorithm allows us to calculate the functional relationship between oviposition dates in one generation and the next. An example of a *G* function for Mountain Pine Beetle, using developmental temperatures collected in the field, appears in Figure 3.

## 4. PROPERTIES OF THE *G* FUNCTION

### 4.1. Shape of the Graph and Biological Interpretation

The *G* function appearing in Figure 3 depicts the general characteristics of oviposition mappings for multistage organisms in temperate thermal regimes. When plotted modulo 365 the graph of the *G* function has both horizontal and vertical asymptotes. The vertical asymptote corresponds to that day beyond which development cannot complete in the same calendar year. The horizontal asymptote corresponds to the earliest possible day of oviposition resulting in a complete generation within the same year. The *G* function is increasing, corresponding to order preservation, which means biologically that an egg laid earlier than another can never mature into an adult later. However, it is not *strictly* increasing; flat spots are possible due to the existence of developmental thresholds. Imagine the following situation: a population of

individuals with differing oviposition dates, developing until they reach a stage with a higher developmental threshold. At this point the earliest individuals are developmentally `stuck' as they wait for temperatures to rise enough to allow development to in the next life stage. In the meantime, individuals oviposited later are still developing, catching up with those individuals stopped at the threshold. When temperatures rise far enough for development to proceed a whole group of individuals with differing oviposition dates are stopped at the entrance to the next life stage, and will be released simultaneously. From a mathematical perspective they are identical, and will have the same emergence date from the final life stage. In the graph of the *G* function this appears as a flat spot, or group of input oviposition dates with the same emergence date.

Jump discontinuities are also possible, caused by the same quiescent period which creates the flat spots. The situation is analogous to traffic moving past a stop light which is red when temperatures are below threshold and green when temperatures are above. Individuals pile up at the light when it is red and are released when it turns green, creating pulses of traffic which generate the flat spots in the *G* function, as described above. However, if traffic is flowing and temperatures drop below threshold, the light suddenly turns red, stopping traffic in midstream. This occurs when a cohort of individuals with nearby oviposition dates are in a high-threshold life stage. Some may be completing development in that stage, others slightly behind, and when temperatures drop below threshold those still in the stage will be stopped while those completing can continue on. Emergence dates for the two sets of individuals, those stopped behind the light and those who just made it through, will be very different, even though they may have had similar oviposition dates. This creates jump discontinuities in the *G* function. There may be as many discontinuities as the number of times temperatures drop below threshold in *any* life stage.

The flat spots created by quiescence can serve as strong synchronizing influences on a population. Immediately on getting stuck at a threshold and allowing a cohort of individuals to catch up a component of the population becomes developmentally identical, in spite of their differing original oviposition dates. This clearly assists with one of the three requisites for an adaptive seasonality: synchrony. Below, when we discuss the dynamic behavior of circle mappings under the *G* function, we will see that the other requisites are enhanced as well.

**4.2. Dynamic Analysis of the *G* Function**

The timing of oviposition from year to year can be viewed as applying the *G* function repeatedly to dates of the year and interpreting the results modulo 365, as illustrated in Figure 4. Each output date from one generation becomes the input date for the next, resulting in a reflection between the mod-365 graph of the *G* function and the fixed point line $t_0^{n+1} = t_0^n$. Where the line and the *G* function cross a univoltine (or possibly other integer voltinism) solution exists, and if the slope at the crossing is smaller than one the fixed point is stable, attracting nearby solutions.

An important consequence of quiescent periods in development, or flat spots in the *G* function, is super-exponential convergence to fixed points. In mappings where the slope of the function is smaller than one but larger than zero, iterates approach the fixed point geometrically in time (e.g. halving the distance at each iteration if the slope is ½) but never actually reach the fixed point. However, if the fixed point occurs at a quiescent flat spot, iterates approach super-exponentially, in a finite number of iterations. This exerts a powerful synchronizing influence on oviposition dates for the entire population, improving the chances of adaptive seasonality.

Another consequence of quiescence is the existence of vertical jump discontinuities caused when a cohort of individuals gets separated by temperatures passing below a

developmental threshold. Dynamically this creates a situation in which a univoltine fixed point can simply disappear without warning. Normally fixed points are created by the crossing of smooth curves, and if the curves cross in one place they must cross in another. This means that fixed points of continuous maps must be created and destroyed in stable and unstable pairs (saddle-node bifurcations in the parlance of dynamical systems theory). However, examining Figure 4 illustrates that there is only one, stable fixed point. The unstable fixed point we might normally expect does not exist because of the discontinuity in the *G* function.

**4.3. Synchronous and Asynchronous Fractional Voltinism**

In the discussion so far we have focused on univoltinism and fixed points of the *G* function interpreted modulo 365, since the timing and synchrony of one generation per year is important for so many organisms in temperate environments. However, other adaptive seasonalities are possible. Many agriculturally important insects go through two or three generations per year (bi- or tri-voltinism), all of which must be timed with crop phenology and resource availability. On the other hand, many important forest insects (for example mountain pine beetle and spruce beetle) exhibit an endemic state in which a single generation completes every two years (semivoltinism). These voltinisms are also natural, structurally stable consequences of circle maps, as we will discuss below.

An elementary dynamical property of order-preserving circle maps is the *rotation number*. The rotation number is the average number of rotations proscribed by points iterated under the circle map. Given the mapping, $t_0^{n+1} = G\left(t_0^n\right)$, for a periodic temperature series and times *not* interpreted modulo 365 (so that the range and domain of *G* are unbounded), the rotation (or winding) number, *W*, is defined mathematically by

$$W = \lim_{n\to\infty}\left[\frac{G^n(t_0)}{365\,n}\right].$$

Here $G^n(t_0)$ denotes the $n$th iterate of $G$, or the oviposition date in the $n$th generation starting with an initial oviposition date of $t_0$. As $n$ grows larger and larger the fraction $G^n/n$ approaches the mean slope of the $n$th generation oviposition curve, giving an average value in terms of number of days per generation. Dividing by 365 gives average number of years per generation, corresponding to the average number of rotations proscribed by oviposition mappings each year. It is not obvious that this rotation number doesn't depend on the choice of initial oviposition date, but the initial point can be shown not to matter using the following argument. If starting with two different points yielded different rotation numbers, then at some point (moving backwards in time) the points would have to be organized so that the more slowly rotating point was in front of the more rapidly rotating point. It then follows that the more slowly rotating point would be passed by the more rapidly rotating and order would no longer be preserved, leading to a contradiction.

Winding number is particularly important in insect development because it corresponds directly to voltinism, or number of generations completed per year. A univoltine life cycle corresponds to a winding number of one, bivoltine to a winding number of two, and semivoltine life cycle gives a winding number of one half. In general, for continuous circle maps, the winding number also indicates what kinds of stable and unstable orbits exist. For rational rotation numbers $m/n$, $m$ and $n$ integers, there is cycles of length $m$, meaning that the equation

$$G^m(t) = \underbrace{G(G(G...G(t)...))}_{m \text{ times}} = t$$

has a root. Each root, $t^*$, corresponds to an orbit of points

$$t^*, G(t^*), G^2(t^*), ....G^{m-1}(t^*),$$

that takes $n$ years to repeat when interpreted modulo 365. Each point in this orbit inherits properties of stability or instability of its parent root, $t^*$, and the map $G^m$. Thus, when the winding number is a rational number without a one in either the numerator or the denominator, individuals at arbitrary starting points will be attracted to one of $m$ points on the stable orbit, out of phase with individuals attracted to other points in the orbit.

It can also be shown that the rational orbits are structurally stable. That is, since they are created by the non-tangential crossing of two curves (in this case the graph of $t$ and $G^m(t)$ modulo 365), small perturbations in parameters and inputs can not alter the fact that the curves continue to cross, though it alters *where* they cross. Once cycles or fixed points are created they therefore persist for some range of parameter values and/or temperature regimes. This includes perturbation away from periodicity via interannual variation in the case of temperatures.

What does this mean for the observable insect life cycles? Firstly, many temperate insects require a univoltine life cycle to be adaptive in their environment. Because of the structural stability of the rational 1/1 winding number corresponding to univoltinism, we can expect to observe univoltinism for a range of temperatures and in spite of the intrinsic genetic variability of the population. This is the case for MPB. Similarly bi- and semi-voltinism should be characterized by existence in bands in parameter space. Outside of these bands adaptive seasonality can break down for a variety of reasons. Orbits can be attracted to cycles with multiple points (for example completing three generations in two years); different portions of the population would be attracted to different points in the cycle, resulting in asynchronous fractional voltinism. The more points in a cycle the more likely some of those points will not correspond to adaptive timing. Food resources may be unavailable, environmental conditions

may be too extreme to proceed with some necessary behavior external to the model (for example, too cold to fly and find mates, etc.). In addition, when a cycle takes too many years to complete, the probability of mortality per individual increases, lowering its utility.

Focusing for a moment on univoltinism, an implicit suggestion of this analysis is that there will be sudden and catastrophic collapses as temperatures shift out of the band creating univoltine fixed points. Is this a consequence of direct temperature control, and if so, could we expect more complex timing mechanisms (diapause or sensitivity to photoperiod) to `rescue' populations leaving a univoltine regime? The answer is no. Direct temperature control is mathematically simple, but any deterministic timing mechanism will generate a *G* function, since each oviposition date is linked predictively to a single emergence date in a given developmental environment. The univoltine bands might be broader, and may well depend on more driving variables (day length, resource availability, etc.) but more complex models will still generate a *G* function and therefore the same array of univoltine behaviors, including bands of adaptive parameters outside of which seasonality will suddenly be lost.

Univoltinism has additional mathematical features. A univoltine fixed point is created when $t+365=G(t)$, or when the *G* function intersects the fixed point line modulo 365. Bi- and tri-voltine solutions (winding numbers of 2/1 and 3/1) will also intersect (two and three times as often, respectively). Both quiescence and diapause introduce regions of zero slope into the *G* function and make univoltinism more likely. If the crossing of *G* function modulo 365 and fixed point line occurs in a region of zero slope the resulting fixed point is superstable. So, while the generations proceeding from individuals laid near a regular fixed point should synchronize geometrically rapidly in time (see Fig. 4), those proceeding from being laid near a super stable

univoltine fixed point will converge to the same oviposition date in a small, finite number of generations. Dynamically this makes for an extremely efficient synchronizing mechanism.

## 5. ADAPTIVE SEASONALITY AND THE MOUNTAIN PINE BEETLE

### 5.1. Biological Background

The Mountain Pine Beetle (*Dendroctonus ponderosae* Hopkins, MPB), an important organism in forest ecosystem dynamics, must emerge as an adult in the appropriate season in order to successfully reproduce. Because their prey, conifers of the genus *Pinus*, have chemical defenses against attack, MPB must arrive at trees *en masse* in order to successfully overcome these defenses and lay eggs (Borden 1974). Individual probability of mortality diminishes during a synchronized attack, since success depends on sufficiently high *rates* of attack (Berryman and Raffa, 1987). Since offspring are only produced subsequent to successful attacks, synchronous emergence promotes individual fitness. This requires that the beetles not only emerge as adults at the right time of the year (timing), but also that the beetles emerge essentially all at once (synchrony) (Amman and Schmitz 1988). Both appropriate timing and synchrony are required for an adaptive seasonality. A MPB generation usually completes in one year, although two years may be required at higher elevations (semi-voltinism). Observations indicate that, while eggs may be laid over a 2-3 month period of time, peak adult emergence typically occurs over a much shorter interval (Amman and Cole 1983; Raffa 1988). This suggests that MPB have some mechanism which helps synchronize their emergence. However, extensive rearing of MPB under controlled conditions has shown no evidence of diapause. MPB raised in constant temperature environments emerge at times predicted by rate curves, indicating no necessary secondary cues relating to photoperiod. The principle of parsimony suggests that phenology is

under direct temperature control, and the theory developed above should apply. Nonlinear growth rate curves based on an initial parametrization by Logan and Amman (1986), extended to later life stages by Bentz et al. (1991) for a simulation model, and fully described in Powell et al. (2000) are depicted in Figure 5.

### 5.2 Outbreak and Univoltinism in the Ghost Forests of Central Idaho

As an example application of the *G*-function theory, we consider a long-term mountain pine beetle study site established on Railroad Ridge, in the White Cloud Mountains of Central Idaho. This site is more fully described in Logan and Powell (2001), but briefly, it is a high elevation site (10,000 ft.) that provides an ideal whitebark pine habitat. Whitebark pine (*Pinus albicaulis* Engelmann) is one of several five-needle pines that grow at high elevation in the Rocky Mountains. These pines are long-lived species that are not particularly adapted to outbreak insect disturbances (in contrast to some pines, e.g. lodgepole pine, which incorporate such disturbances in their reproductive strategy [Amman and Schmitz 1988]). In fact, one explanation for the distribution of the high-elevation, five needle pines is an escape strategy from the host of insect pests and pathogens that occur in more benign environments. Unfortunately, these pines face a variety of anthropogenic threats including introduced pathogens and the effects of global warming. Our objective in this example is to illustrate application of *G*-function analysis for a potential pest species invasion of a sensitive habitat.

We begin by performing a bifurcation analysis of MPB seasonality for micro-habitat phloem temperatures recorded at our North site on Railroad Ridge (Figure 6). This analysis (Figure 7) is obtained by initiating oviposition on some reasonable but arbitrary date (in this case August 1), allowing the model to run for fifty transient generations and then plotting the next

twenty ovipositional dates modulo 365. If all of the last twenty dates are the same, only one point appears, indicating the existence of one generation for an integral number of years. The appearance of two or more points indicates a periodic orbit and either fractional (e.g. semi-) or asynchronous fractional voltinism. We chose twenty for the final plotting procedure simply to verify that the more simple cycles (i.e. with 4 and 5 points) are stable; fifty transient generations was chosen empirically. Since our goal is to examine the persistence of ovipositional fixed points of both simple and fractional voltinism, this iterative approach to determining the fixed points is much simpler than calculating the entire *G* function (as well as its iterates) and searching for fixed points.

This procedure is followed for temperatures obtained by adding $\Delta T$ to each observed hourly temperature of the original 1995 temperature series. As noted earlier, an attracting fixed point is analogous to synchronous emergence while an orbit of ovipositional dates indicates lack of synchrony. As shown in Figure 7, regions of synchronous emergence are separated by regions of asynchrony. Exploring the adaptive seasonality of the observed temperature cycle ($\Delta T = 0$), we note that one of the necessary conditions, synchrony, has been met as indicated by the pair of intersections of the *G*-function with the fixed-point line shown in Figure 8.

The other necessary conditions are revealed by plotting a graph of the winding function (Figure 9). The winding function is a plot of the last twenty iterates of the *G*-function, as in Figure 7, but in polar coordinates. A complete revolution occurs in exactly one year (measuring from an angle of zero from the vertical being midnight, December 31, and the distance from the origin is given by picking a radial distance equal to the fraction of a year completed by the cycle (i.e. an exact univoltine orbit proscribes one revolution and will end up one unit further from the origin than its starting point). Examining Figure 9 we see that while one of the remaining

necessary conditions for adaptive seasonality is met, i.e. oviposition at an acceptable time of year, the remaining condition (univoltism) is not. The orbit proscribes two revolutions, meaning that the life cycle in this thermal environment is semivoltine (two years per generation). This result for high elevation environments is consistent with the observations of Amman 1973, and Safranyik (1978), who noted elevational zones of climatic adaptation where MPB was univoltine in lower elevation, lodgepole/ponderosa pine zones, exhibited mixed voltinism at intermediate elevations, and was semi-voltine at high elevations. These authors further observed that univoltinsm was essential for MPB to reach outbreak densities. MPB are semivoltine in thermal regimes corresponding to the 1995 Railroad Ridge temperatures, and therefore unable to achieve outbreak densities, though they may be able to maintain endemic populations.

The *G*-function obtained by adding 1°C to each hourly temperature is shown in Figure 10. The lack of intersection of the *G*-function with the fixed point line indicates no fixed points. The cobwebs in Figure 10 indicate a ten point orbit, taking four years to complete, and some points on the orbit occur at dangerous times of year. As described earlier, different initial oviposition dates will be attracted to different points on the orbit, resulting in a lack of synchrony. The same holds for any temperature regime in regions of fractional voltinism in Figure 7. In other words, warming of the observed mal-adapted semivoltine temperature cycle of 1995 would *reduce* the suitability of the habitat.

Increasing mean annual temperature by 3°C results in the *G*-function shown in Figure 11. The intersection of the *G*-function with the fixed-point line indicates that univoltine synchrony has been restored at an acceptable time of year. The ecological interpretation is that increasing mean annual temperature by 3°C transformed a mal-adapted thermal habitat into an adaptive thermal habitat. An increase of this magnitude is well within model predictions for global

warming anticipated by mid-century, with obvious implications for high-elevation pines. Looking backwards in time, a major outbreak of MPB in Idaho's high-altitude white bark pine occurred in the early 1930s, which was also the only time in the previous century that mean summer temperatures were more than 2.5°C above century averages (Logan and Powell 2001).

The theoretical framework behind *G*-function analysis provides a powerful way to evaluate thermal ecology for a specific weather pattern or climate. Understanding the dynamical properties behind the bifurcation analysis of Figure 7 enhances ecological interpretation. A simplistic understanding suggests that monitoring MPB dynamics in high elevation systems could provide a good indication of climate change because it integrates complex climate signals into a measurable and observable phenomenon, MPB outbreak. However, a more in-depth analysis of the dynamical properties of MPB phenology indicates this might not be the case. Thermal conditions for the beetle do not necessarily improve in a continuous fashion. The thermal habitat may actually become less hospitable until a threshold is reached, and then suddenly become much more hospitable, leading to catastrophic impacts with little or no warning (Logan and Powell 2001).

**5.3. Attack Success in the Stanley Valley during the Pinatubo Perturbation**

As a second example of *G*-function application, consider the Stanley Basin study site in Central Idaho where we have maintained intensive research on mountain pine beetle population dynamics for almost 15 years. This area includes the headwaters of the Salmon River and the Sawtooth National Recreation Area. In addition to some of the most spectacular scenery in North America, the Stanley Basin provides a unique opportunity for research involving mountain pine beetle dynamics. It is well within the geographic distribution of the beetle and contains ample forests of lodgepole pine. Due to meso-climatic reasons, the thermal habitat is historically

only marginally suited for MPB. This has two important results: first, instead of the dramatic boom-and-bust outbreak cycles of more suitable climates, historical populations tend to be maintained at sub-outbreak levels for prolonged periods. This has allowed for detailed population dynamics research at one site for a prolonged time. Second, climate marginality means that slight variation in annual weather patterns result in immediate and measurable population responses. See Logan and Bentz (1999) for a more detailed description of the Stanley Basin in relation to mountain pine beetle ecology. In spite of the historic marginality of the climate from the MPB perspective, the last eight years (1995-2003) have seen an outbreak of major proportions growing in this area.

As an indication of the sensitivity of the mountain pine beetle population response to weather in the Stanley Basin, consider the annual attack densities from the USDA-FS annual Aerial Detection Survey (ADS) data (Figure 12). ADS data is collected by flying over a region in a light aircraft and noting areas with red-topped lodgepole pine on a digital sketch pad with a mapping data base. Polygons formed must enclose at least ten impacted trees but may also include regions with complete mortality. The sketch maps are therefore difficult to convert into actual numbers of attacked trees, but give a good indication of total area impacted by MPB. From Figure 12 it is apparent that large areas of forest were impacted in 1991-92, but the pulse of larvae resulting from these attacks generated very few successful attacks the following summer (1993). During the summer of 1994 the successful attack cycle was reinitiated, although at a reduced level resulting from the population depression the occurred in 1993. Subsequent, warmer years saw ever-increasing population growth, as indicated in Figure 13. As it turns out, the summer of 1993 (depressed population) was the coldest summer (June, July, August) on record due to the Pinatubo eruption Extreme winter temperatures are a major mortality factor for

mountain pine beetle populations (Cole 1975). Winter temperatures for 1992-1993 were only moderately colder than average, far from the record setting event of summer 1993. As an alternative to unusually harsh winter temperatures, we hypothesize that the cool summer of 1993 interfered with the adaptive seasonal patterns that existed both before and after 1993.

The impact of lowered summer temperatures is evident in the *G*-function resulting from annual phloem temperatures recorded at our Ranch site, Stanley Basin for 1993. The *G*-function (Figure 14) indicates a maladaptive seasonality: the curve lacks a synchronizing fixed point, oviposition periods occur too late in the year, and emergence times are inappropriate. In contrast, consider the dynamics of the *G*-function resulting from 1995 temperatures recorded at the same site (Figure 15). Temperatures from 1995 were more typical for the Stanley. From this *G*-function we see that an intersection with the fixed-point line occurs and that the attractor is at an appropriate time of year, indicating an adaptive annual weather cycle. The bifurcation plot resulting from 1995 temperatures (Figure 16) indicate that observed temperatures are at the leading edge of a univoltine, adaptive temperature regime. This is in keeping with the historic interpretation of marginal thermal habitat in the Stanley Basin. Although the resulting seasonality is adaptive, small negative perturbations to temperature will make it nonadaptive. On the other hand, if temperatures continue to warm, moving toward the middle of the adaptive band, resiliency to variability in temperature will increase and the likelihood of favorable years for MPB will also be increased.

If we consider 1995 as an "average" weather year, the implication is that warming temperatures will result in improved thermal habitat for the mountain pine beetle. Temperatures for NCDC Division 4, including the Stanley Basin, show a steady increasing trend in annual mean beginning somewhere around 1980 (Figure 17). If this trend continues, our model

predictions are for an increasing proportion of years that are favorable for mountain pine beetle populations, shifting the Stanley Basin from a low- or moderate- to high-hazard area. (see Safranyik's (1978) definition of a "high-hazard" area).

## 6. DISCUSSION AND CONCLUSION

Climate changes, like the steady temperature increase observed in the Stanley Basin over the past twenty years, are likely to be the norm instead of the exception (Houghton et al 1990). We have presented an integrated dynamical viewpoint on the interaction between one aspect of climate (temperature) and poikilothermic life cycles. Nonlinear circle maps, which intimately relate the circularity of life histories and the periodicity of yearly temperature signals, naturally generate stable, attracting fixed points and orbits in broad thermal bands. These attractors are structurally stable, meaning that they persist for small changes in temperature and life history parameters. Thus they can serve to organize and synchronize populations for appropriate emergence.

For temperate insects, and particularly the mountain pine beetle, ecological success is correlated with adaptive seasonality: timing of life cycle events for appropriate times of year, univoltinism, and simultaneous emergence of cohorts across the landscape. Fixed points in the *G*-function circle map automatically satisfy two of these three requisites (univoltinism and synchrony). Since it is simple to check the fixed points for appropriate timing, the *G*-function provides a powerful theoretical tool for understanding the adaptation of a population to its thermal environment. As discussed above, the effect of univoltine fixed points (or lack thereof) is felt almost immediately in the population and can be used to understand even one-time perturbations like the Pinatubo eruption.

Broader consequences of this viewpoint merit further attention. In particular, univoltinism can be lost immediately instead of gradually as temperatures move outside of a

band of thermal adaptation. It might seem that secondary emergence cues, for example sensitivity to photoperiod or delaying emergence if daily temperatures are not sufficiently warm, might serve to save a population from the consequences of losing univoltinism. However, such mechanisms, being deterministic, simply lead to a slightly different *G*-function. Secondary cues or more complicated timing mechanisms may lead to different bands of univoltinism, but these new bands will still have end points at which synchrony is lost catastrophically.

Two corollaries suggest themselves. For native insects whose adaptation to environment depends on timing, we predict that long term temperature changes in any direction will eventually cause univoltine timing to vanish. Distressingly, when univoltinism vanishes it vanishes suddenly as opposed to gradually. Thus we may expect local populations to `wink out' suddenly and with little warning. Conversely, thermal habitats that are only marginally at risk for outbreaks may suddenly become much more susceptible, as in the case of the high altitude white bark pines stands of the Rocky Mountains (Logan and Powell 2001). Secondly, for exotic species historic guidelines on climate matching may be no guide to habitat suitability. Adaptive thermal bands can suddenly `pop' into existence as a consequence of climate change, and if an introduction of an exotic species occurs at such a time the population may be able to establish and spread, even if historic introductions have failed.

We have not considered here the effect of diapause, and a broad spectrum of poikilothermic organisms exhibit some form of diapause, either facultative or obligatory. In broad strokes, the *G*-function approach should still apply; for every possible input time of year there is a unique output time of year for the median individual, and thus a *G*-function exists and can be used to examine adaptive seasonality. Recent work (Regniere and Nealis 2003) is based on predicting the voltinism of diapausing insects, although the *G*-function concept is not used

explicitly. Modeling progression through individual life phases may become much more complicated, requiring models of higher dimension than the single rate curve models above. Generally, the effect of diapause is to increase resiliency to weather variation, but at the cost of reduced adaptability. In the absence of diapause, the location of thermally adaptive bands is free to move geographically and the population is free to move with it (as the mountain pine beetle is now moving into previously unoccupied regions of British Columbia [Carroll et al. 2003]).

An additional area of interest is the effect of variability in phenotype. Laboratory experiments designed to parameterize rate curves universally indicate some degree of variance in individual rates of development about the median; some individuals age more rapidly, others age more slowly, even in a constant temperature environment. The *G*-function approach is explicitly based on the behavior of the median individual. Since the existence of univoltine fixed points is structurally stable, for small degrees of phenotypic variance we can expect the scenarios described here to hold. In fact, a certain degree of variability should actually broaden the thermal bands of adaptivity. As the edges of an adaptive band are approached, some individuals in a population will always be slower or faster, making the edges of the band a bit further out for them and insulating the population at large from complete collapse. Thus phenotypic variability could function as a bet-hedging strategy at the population level, insuring some degree of viability in the face of thermal variability. More quantitative statements will have to wait on the examination of models which realistically relate variability, development and temperature in the light of the *G*-function perspective presented here.

**Acknowledgements**

Research presented here was supported by the National Science Foundation of the United States under grant number DMS 0077663.

**Literature Cited**


- Amman GD. 1973. Population changes of the mountain pine beetle in relation to elevation. Environmental Entomology 2:541-547.
- Amman GD, and Schmitz RF. 1988. Mountain pine beetle – lodgepole pine interactions and strategies for reducing tree losses. AMBIO 17:62-68.
- Amman GD, and Cole WE. 1983. Mountain pine beetle dynamics in lodgepole pine forests part II: population dynamics. USDA Forest Service General Technical Report INT-45
- Battey NH. 2000**.** Aspects of seasonality. Journal of Experimental Botany 51:1769-1780.
- Bentz BJ, Logan JA, Amman GD. 1991. Temperature dependent development of mountain pine beetle and simulation of its phenology. Canadian Entomologist 123:1083-1094.
- Borden JH. 1974. Aggregation pheromones in the Scolytidae. Pages 135–160 *in* , M. C. Birch, ed. Pheromones. North-Holland, Amsterdam.
- Carroll AL., Taylor SW and Régnière J. 2003. Climate change and range expansion by the mountain pine beetle: tomorrow's problem or today's reality. Canadian Entomological Society Symposium Proceedings (in press).
- Cole WE. 1975. Interpreting some mortality interactions within mountain pine beetle broods. Environmental Entomology 4:97-102.
- Danks HV. 1987. Insect dormancy: an ecological prospective. Monograph Series No. 1. Biological Survey of Canada (Terrestrial Arthropods), Ottawa.
- Grist EPM and Gurney WSC. 1995. Stage-specificity and the synchronisation of life-cycles to periodic environmental variations. Journal of Mathematical Biology 34: 123-147.

- Gurney WSC, Crowley PH, and Nisbet RM. 1992. Locking life cycles onto seasons: Circle-map models of population dynamics and local adaptation. Journal of Mathematical Biology 30: 251-279.
- Gurney WSC, Crowley PH, and Nisbet RM. 1994. Stage-specific Quiescence as a Mechanism for Synchronizing Life Cycles to Seasons. Theoretical Population Biology 46:319-343.
- Hill JK, Thomas CD, Huntley B. 1999. Climate and habitat availability determine 20th century changes in a butterfly's range margin. Proceedings of the Royal Society Series B Biology 226: 1197-1206.
- Janisch, E. 1932. The influence of temperature on the life history of insects. Transactions of the Entomological Society of London 80:137-168.
- Houghton JT., Jenkins GT, and Ephraums JJ, eds. 1990. Climate change: the IPCC scientific assessment. Cambridge University Press, Cambridge, UK.
- Logan JA. 1988. Toward an expert system for development of pest simulation models. Environmental Entomology 17**:**359-376 (1988).
- Logan, JA and Amman GD. 1986. A distribution model for egg development in mountain pine beetle. Canadian Entomologist 118:361-372.
- Logan JA and Bentz BJ. 1999. Model analysis of mountain pine beetle seasonality. Environmental Entomology 28: 924-934.
- Logan JA and Powell JA. 2001. Ghost forests, global warming, and the mountain pine beetle. American Entomologist 47:160-173
- Logan JA, Regniere J and Powell JA. 2003. Global warming and forest pest dynamics. Frontiers in Ecology and the Environment 1:130-137.

- Logan JA., Wollkind DJ, Hoyt SC and Tanigoshi LK. 1976. An analytic model for decription of temperature dependent rate phenomena in arthropods. Environmental Entomology 5:1133-1140.
- Menzel A, and Fabian P. 1999. Growing season extended in Europe. Nature 397:659.
- Powell J., Jenkins J, Logan JA, and Bentz BJ. 2000. Seasonal temperature alone can synchronize life cycles. Bulletin of Mathematical Biology 62:977-998.
- Raffa, KF. 1988. The mountain pine beetle in Western North America. Pages 505-530 *in* A. A. Berryman, ed. Dynamics of Forest Insect Populations: Patterns, Causes, Implications. Plenum, New York.
- Raffa KF and Berryman AA. 1987. Interacting selective pressures conifer-bark beetle systems: a basis for reciprocal adaptation? American Naturalist 129:234-262.
- Reid RW. 1962. Biology of the mountain pine beetle *Dendroctonus ponderosae* Hopkins, in the Kootenay Region of British Columbia. I. Life cycle, brood development and flight periods. The Canadian Entomologist 94: 531-538.
- Régnière J and Nealis V. 2003. Modeling seasonality of the gypsy moth, *Lymantria dispar* L. (Lepidoptera: Lymantriidae) to evaluate the persistence in novel environments. Canadian Entomologist 134:805-824.
- Safranyik L. 1978. Effects of climate and weather on mountain pine beetle populations. Pages 77-84 *in* A. A. Berryman, G. D. Amman, and R. W. Stark, eds. Theory and practice of mountain pine beetle management in lodgepole pine forests. Symposium Proceedings, University of Idaho, Moscow, Idaho.
- Safranyik l, and Whitney HS. 1985. Development and survival of axenically reared mountain pine beetles, *Dendroctonus ponderosae* (Cloeoptera: Scolytidae). The Canadian

Entomologist 117: 185-192.

- Samman, S. and J.A., Logan (Eds.) 2000. Assessment and response to bark beetle outbreask in the Rocky Mountain Area. USDA Forest Service Technical Report, RMRS-GTR-62.
- Sharpe PJH, and DeMichele DW. 1977. Reaction kinetics of poikilotherm development. Journal of Theoretical Biology 64:649-670.
- Stinner RE, Butler GD, Bacheler JS and Tuttle C. 1975. Simulation of temperature dependent development in population dynamic models. The Canadian Entomologist 97:1167-1174.
- Wagner TL, Wu H-I, Sharpe PJH, Schoolfield RM and Coulson RN. 1984. Modeling insect development rates: a literature review and application of a biophysical model. Annals of the Entomological Society of America 77:208-225.
- Wang JY. 1960. A critique of the heat unit approach to plant response studies. Ecology 41:785-790.
- Wygant, N. D. 1942. Effects of low temperature on the Black Hills Beetle (*Dendroctonus pondersoae*) Unpublished Forest Service Report. USDA Forest Service, Rocky Mountain Forest and Range Experiment Station (currently the Rocky Mountain Research Station), Ft. Collins, Colorado.

**Table 1.** List and description of parameters, variables and functions.

| Variable/Parameter | Description |
|---|---|
| $j$ | Integer index of organism life stage |
| $a_j(t)$ | `Age' in life stage $j$, or fraction of $j$th life stage completed at time $t$ |
| $N$ | Number of life stages in life history of organism |
| $r_j(T)$ | Developmental rate in stage $j$ as a function of temperature ($T$) |
| $t_j$ | Time (Julian day) at which median individual completes life stage $j$ |
| $t_0^n$ | Time (Julian day) of oviposition for median individual in generation $n$ |
| $G(t)$ | `$G$-function,' Julian day of oviposition of adult developing from an egg laid on Julian day $t$ in previous generation |
| $t^*$ | Fixed point determined by matching oviposition dates in one year and the next |
| $R_j(t)$ | Cumulative developmental integral; total development occurring between times 0 and $t$ |
| $T(t)$ | Temperature in developmental environment as a function of time $t$ |
| $T_0$ | Mean yearly temperature for a sinusoidal temperature model |
| $T_1$ | Amplitude of yearly seasonal temperature swing in a sinusoidal temperature model |
| $\Delta T$ | Temperature increment added to mean temperature in bifurcation analyses of voltinism arising from temperatures in field environments |
| $\rho_1, \rho_2$ | Constants in first and second stages for simple developmental rate functions |
| $\theta_1, \theta_2$ | Temperature thresholds for development in first and second life stages for simple developmental rate functions |
| $W$ | Winding number, or average rotation caused by G function mapping oviposition dates around the circle of yearlydates |

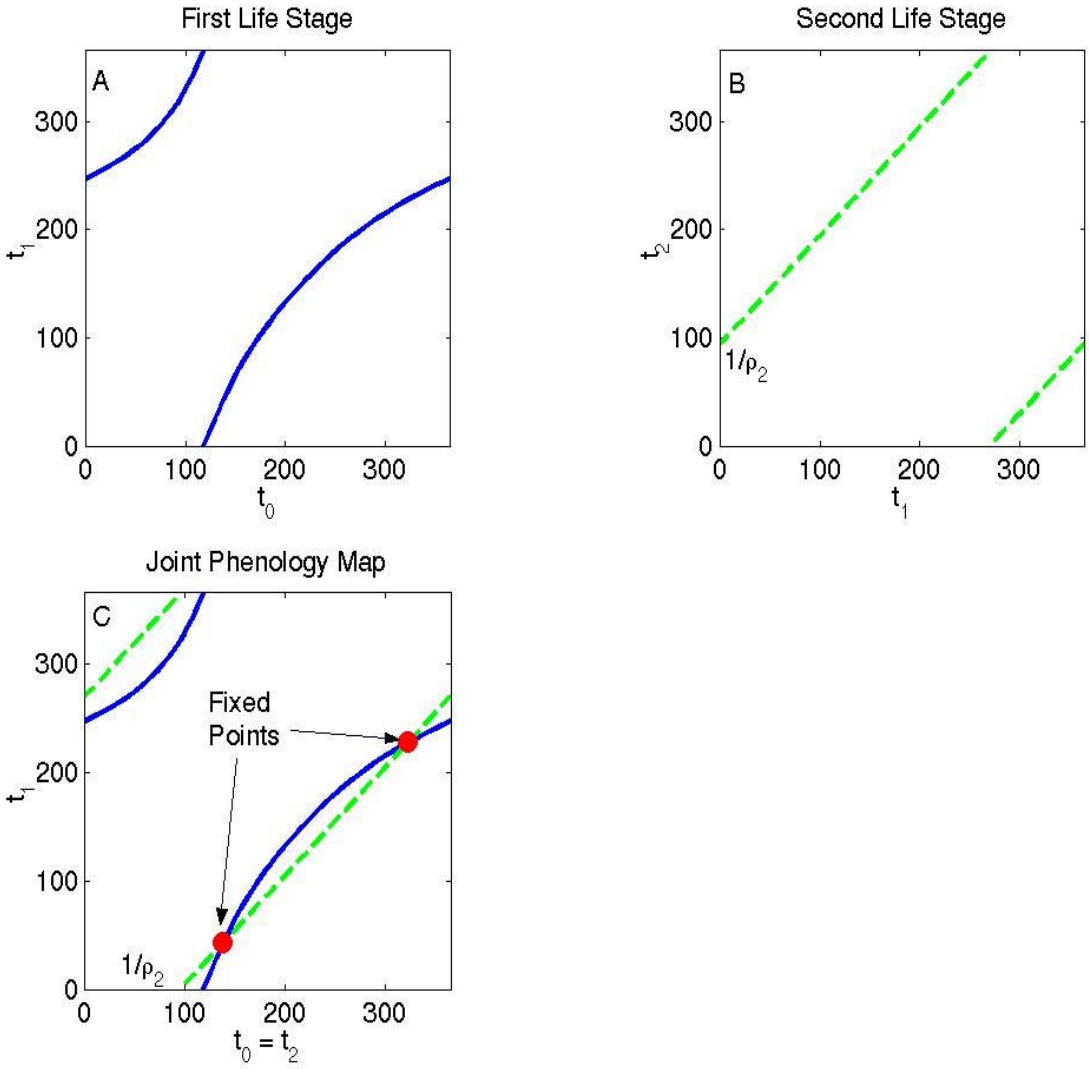


**Figure 1**. Graphical representation of a simple two-stage phenology model, with output from the first stage graphed as solid lines (A), second stage output graphed as dashes (B), and the two graphs merged via identifying $t_0 = t_2$ from the second graph, resulting in an interchange of axes and the reflected plot of second stage output, appearing as a dashed line in (C). Where the dashed and solid curves intersect a univoltine solution exists, indicated by the solid fixed points in the graph at left. Units on both horizontal and vertical axes are Julian Days.

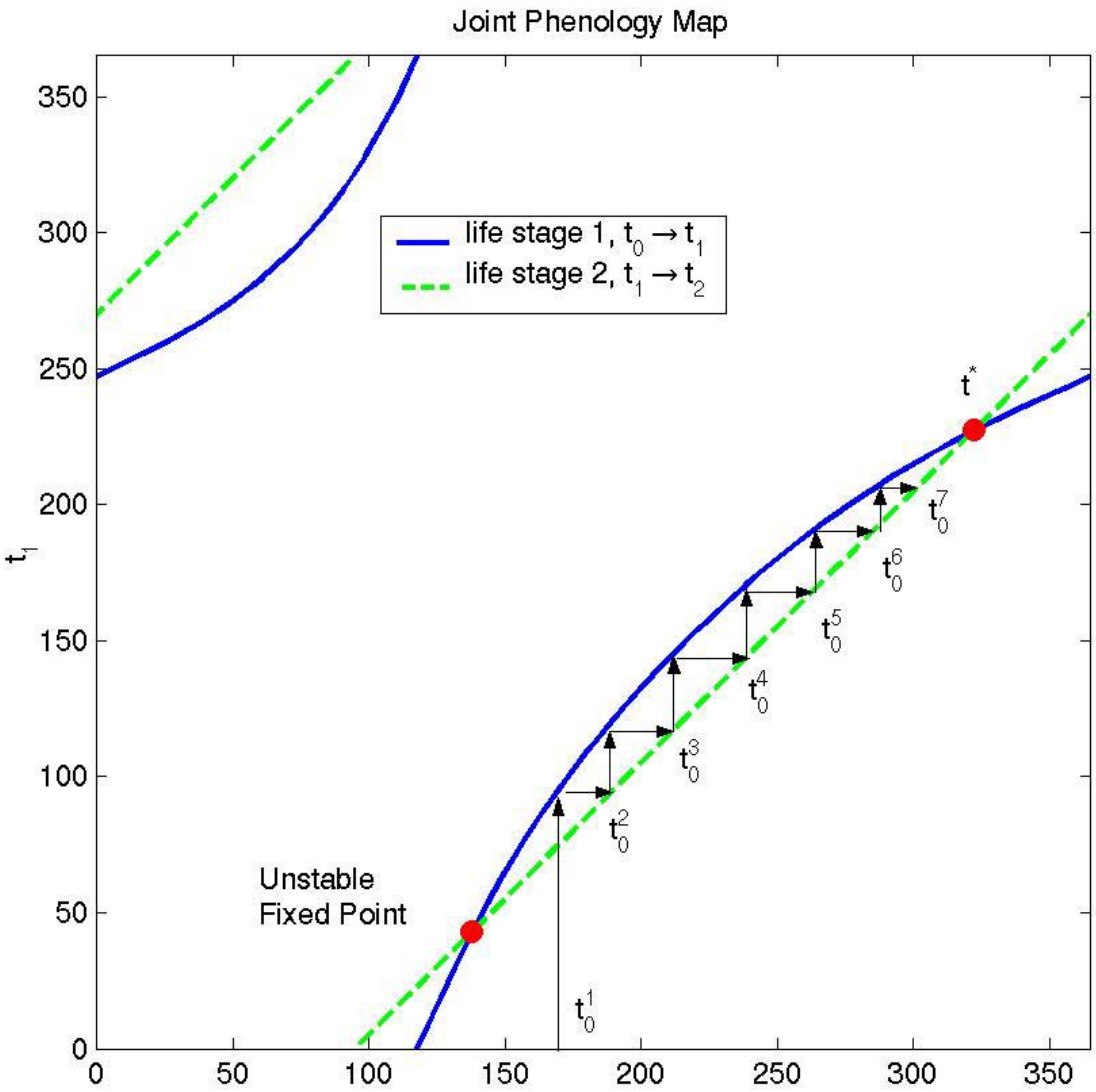


**Figure 2**. Cobwebbing between first and second life stage curves to illustrate the dynamics of the joint two stage phenology map. Julian Day of emergence and oviposition appear on the horizontal axis, while Julian Day of egg hatching appears on the vertical. A sequence of oviposition dates is generated by successive reflections between the first life stage output curve (solid) and the reflected second life stage output curve (dashed). A complete iteration from one generation to the next is accomplished by moving vertically from a given oviposition date to the solid curve (giving by its vertical displacement the output date from the first life stage) and then moving from that point horizontally to the dashed curve (giving by its horizontal displacement the output date from the second life stage). In this case any sequence of oviposition dates will converge to the stable univoltine solution indicated by $t^*$. The other, unstable univoltine fixed point separates initial conditions between those which will converge to $t^*$ from above and below.

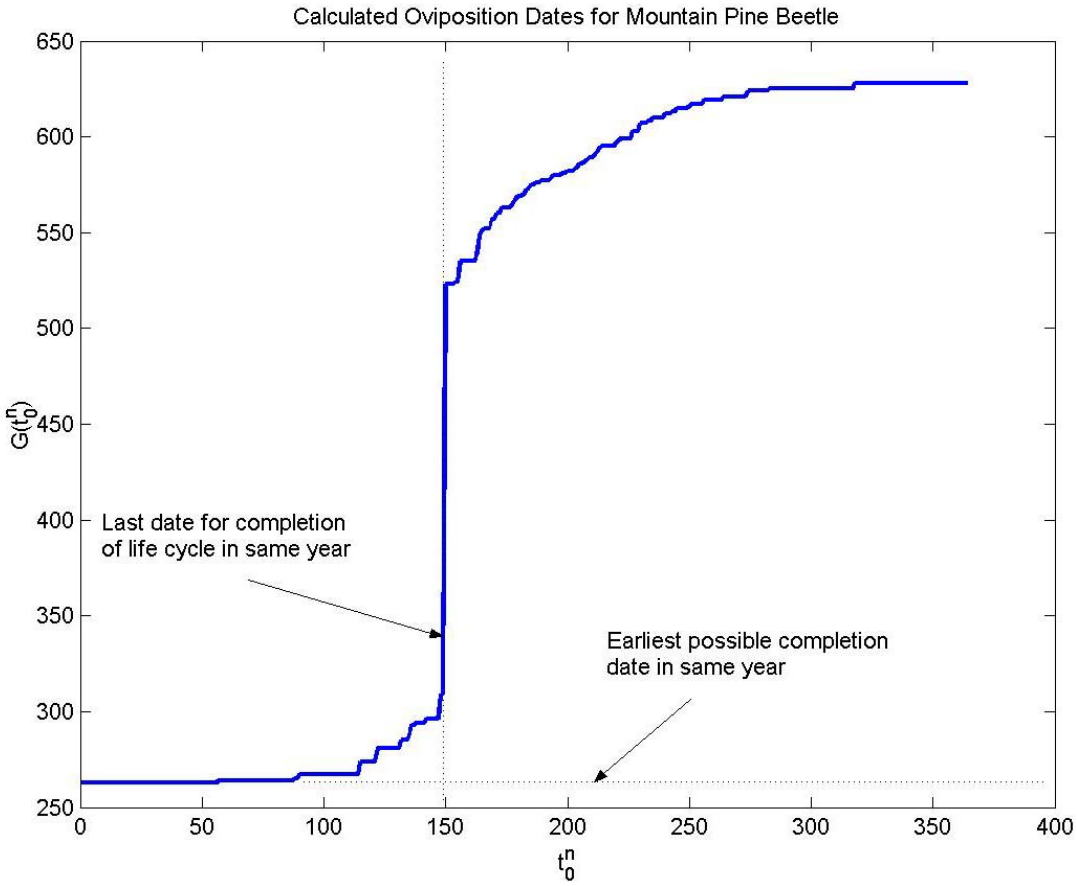


**Figure 3**. Example *G* function for Mountain Pine Beetle, calculated using recorded phloem temperatures in the Sawtooth National Recreation Area of central Idaho from 2002. Julian date of oviposition is plotted on the horizontal axis, and the number of days later that oviposition occurs appears on the vertical axis. The vertical asymptote around day 150 corresponds to the last date during 2002 for which an entire life cycle could be completed in the same year; the horizontal asymptote corresponds to the earliest possible emergence date in that year.

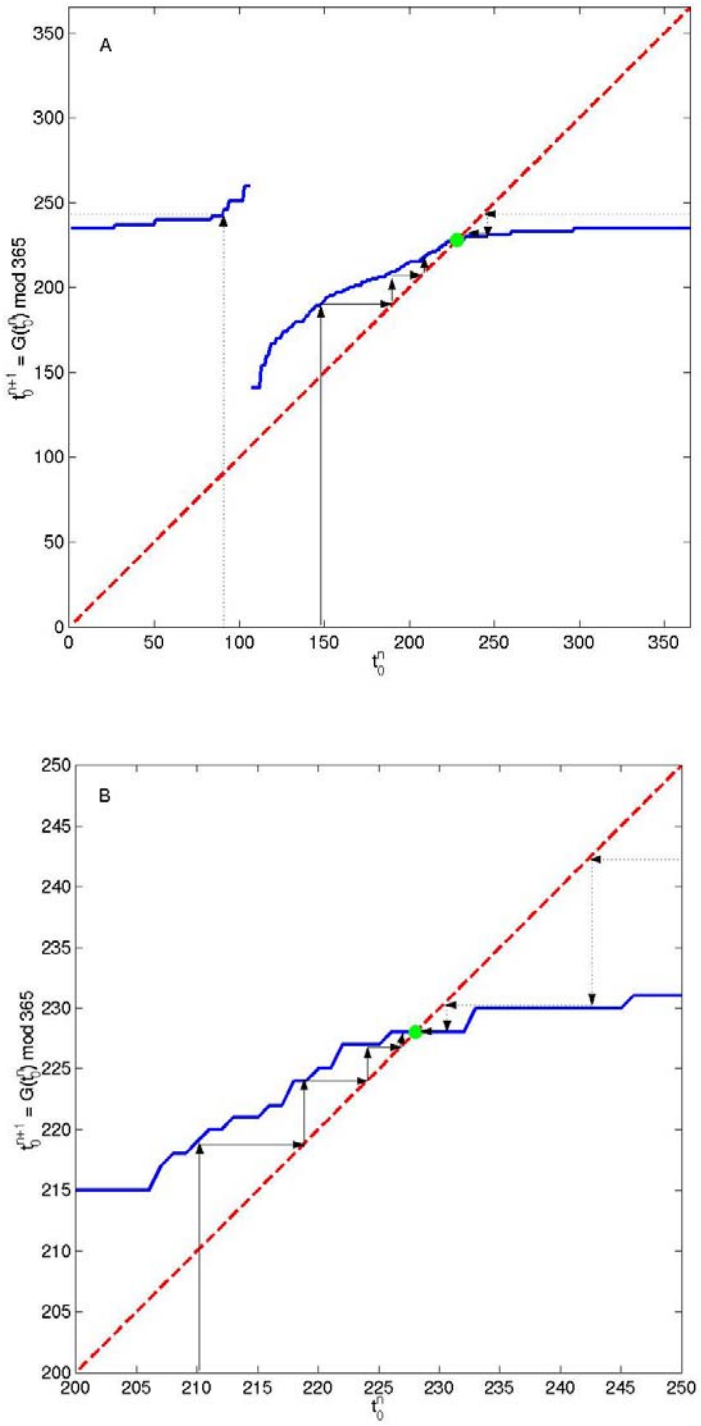


**Figure 4**. Cobwebbing to illustrate the dynamic properties of the *G* function. Julian Day of oviposition in generation *n* and *n+1* are plotted on horizontal and vertical axes, respectively. The solid curves above are oviposition dates in the next generation for given oviposition dates in the previous generation, plotted modulo 365. The dashed line is the $t_0^{n+1} = t_0^n$, and where it crosses the *G* function a univoltine fixed point exists, indicated by the solid circle. Dynamic iteration of the circle map results in reflections between the dashed and solid curves, as indicated by the arrows above. Two trajectories are illustrated, one in dotted and one in solid arrows, illustrating convergence to the fixed point from above and below. The second graph, B, is a blow-up of A for a range of dates close to the fixed point, illustrating the super-exponential convergence of trajectories to the fixed point in cases of quiescence (flat spots in the *G* function).

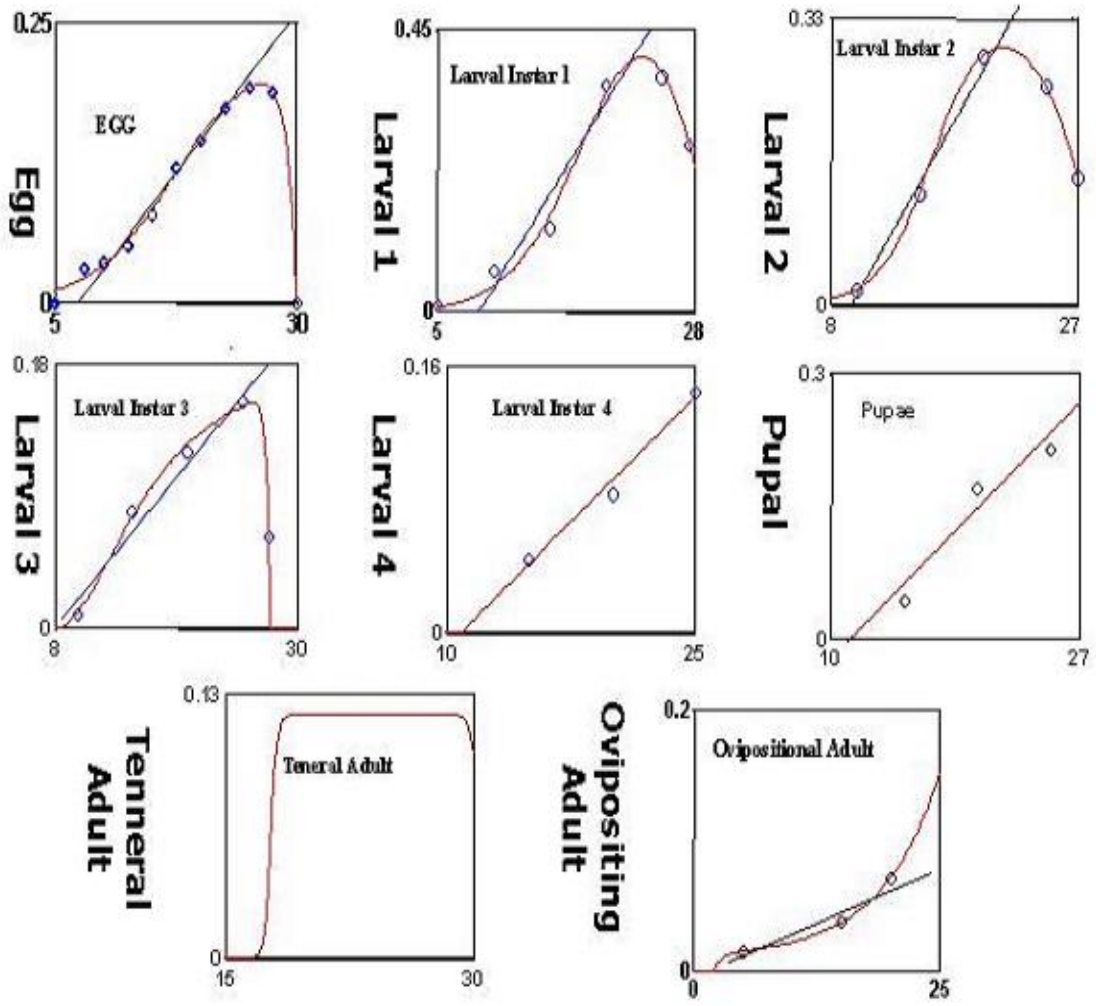


**Figure 5**. Rate curves for the mountain pine beetle. In all curves the vertical axis is measured in development/day and the horizontal axis is temperature in centigrade. Data points determined by rearing at controlled temperatures are depicted as open circles, and in some cases the location of a developmental threshold is estimated by using linear regression on a subset of the data points. Functional descriptions of the curves and best-fit parameter values are discussed in Jenkins et al. 2001.

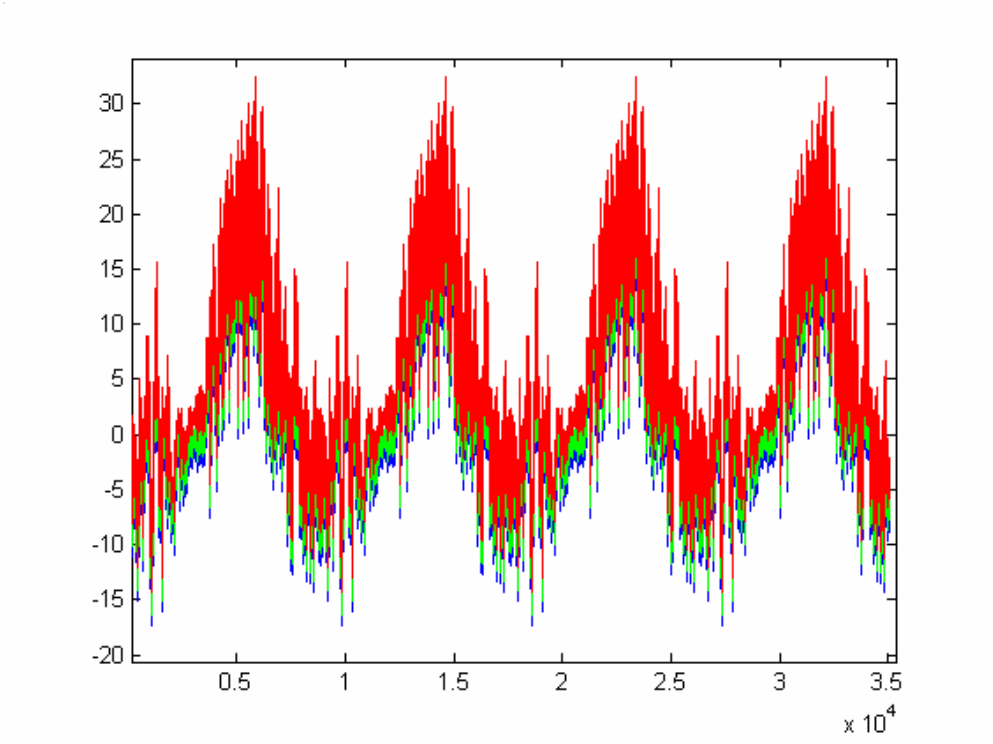


**a**

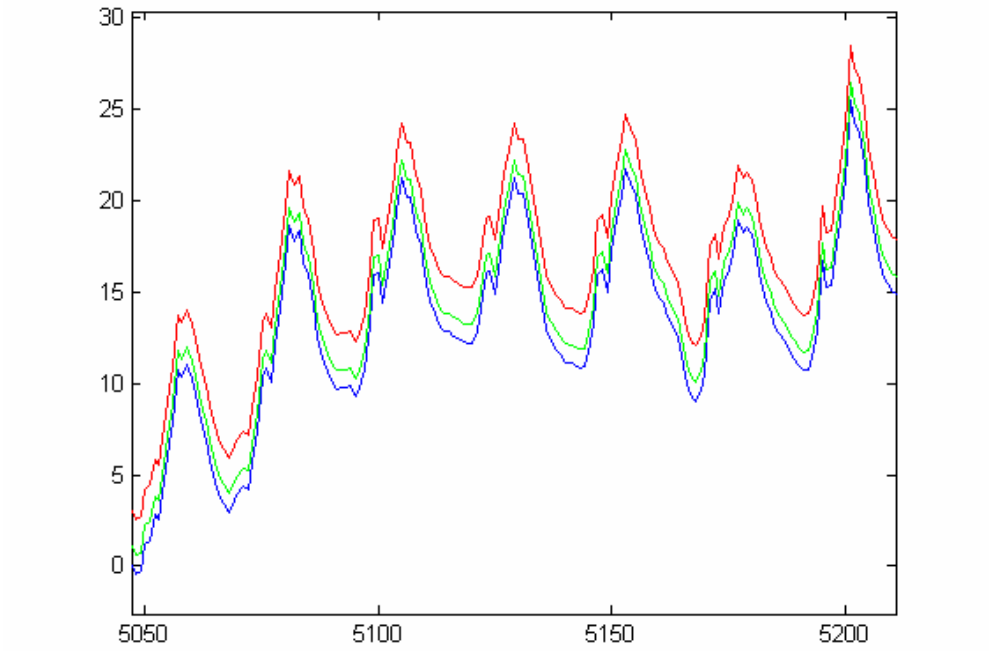


**b**

**Figure 6(a).** Four years of phloem temperatures obtained by repeating the one year average of north and south temperatures recorded a breast height (4 ft.) on a successfully attacked whitebark pine. Horizontal axes are measured in hours, while vertical axes appear in degrees Centigrade. Blue are the observed temperatures, green are the observed temperature + 1.Cº, and red are T+3Cº. It is necessary to measure phloem temperature since our model is parameterized for the temperature experienced by developing larvae, which is quite different from ambient air temperature (Logan and Powell 2001, Fig. 7). **Figure 6(b).** Blowup of the recorded temperatures of (a) for one week of hourly temperatures starting July 29.

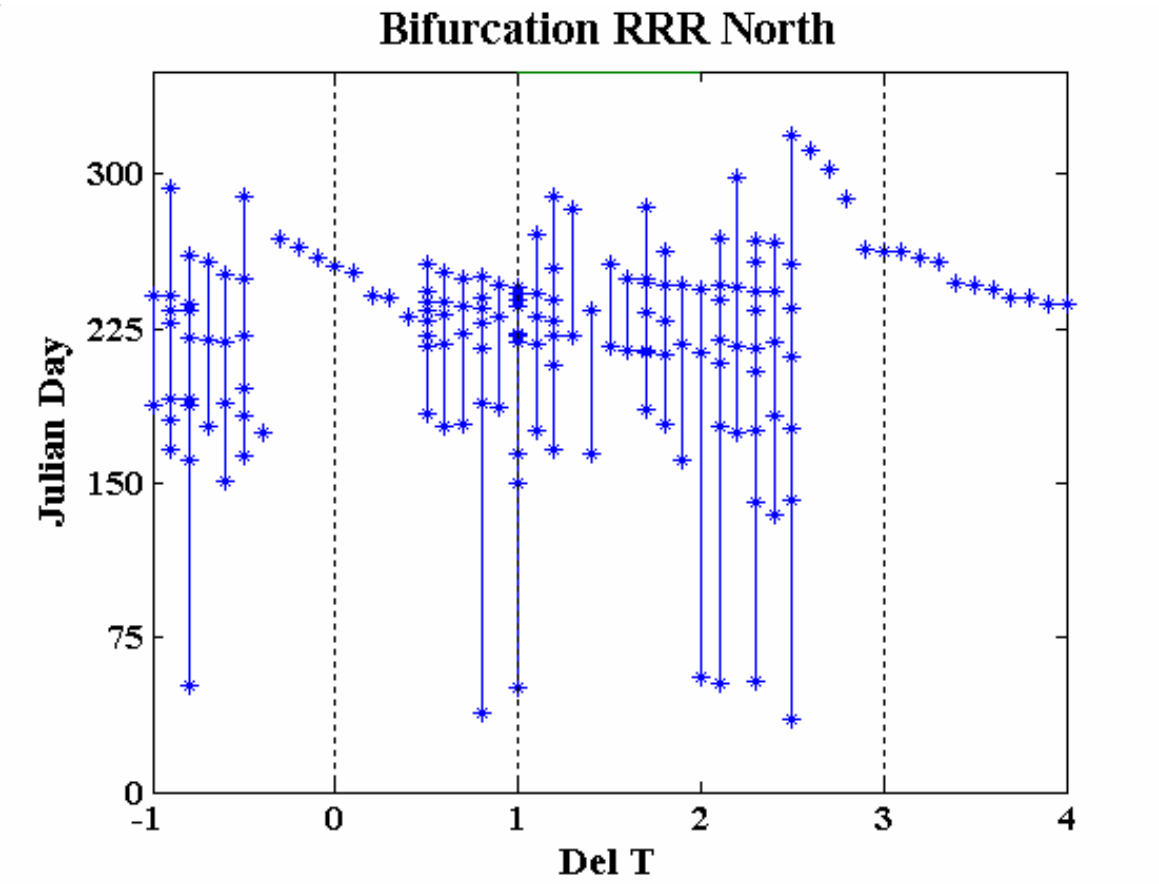


**Figure 7**. Bifurcation plot for the annual temperatures cycle at Railroad Ridge, 1995. On the vertical axis appears Julian day of emergence, while horizontal axis indicates degrees Centigrade added to the 1995 temperature series. The observed temperature (blue in Fig. Ex1.1) is at $x=\Delta T=1$; Increasing the mean annual temperature by 1C° added to each hourly observed temperature (green in Fig. Ex1.1) is indicated by the second dotted line; Increasing the mean temperature by 3C° added to each hourly observed temperature (red in Fig. Ex1.1) is indicated by the third dotted line.

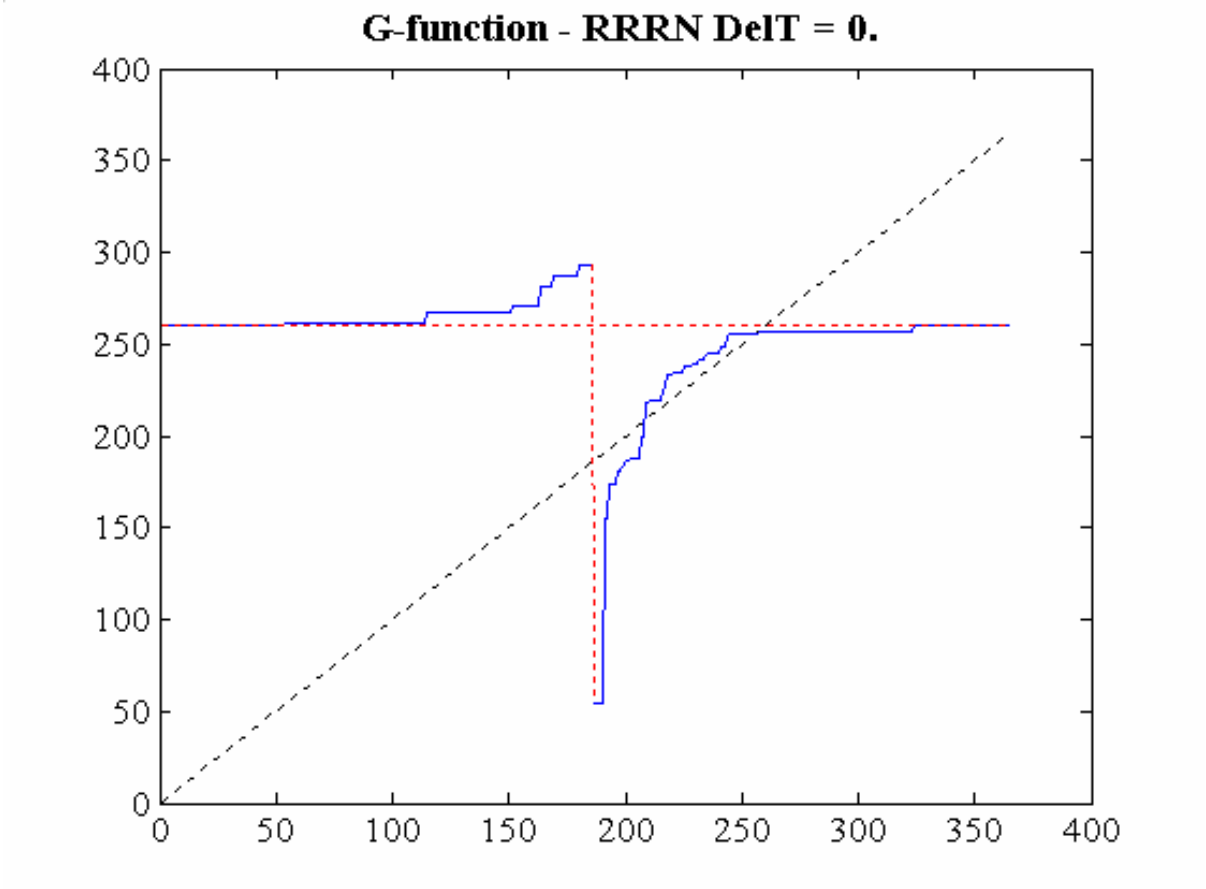


**Figure 8.** *G*-function for the observed cycle of phloem temperatures for Railroad Ridge, 1995. Horizontal axis is input oviposition date for the *n*th generation and the vertical axis is median ovipositional date for the *(n+1)*st generation (reduced modulo 365). Intersections with the dotted 1-1 fixed point line (dashed) indicate fixed points. In this case the stable fixed point occurs around JD 250, in early September.

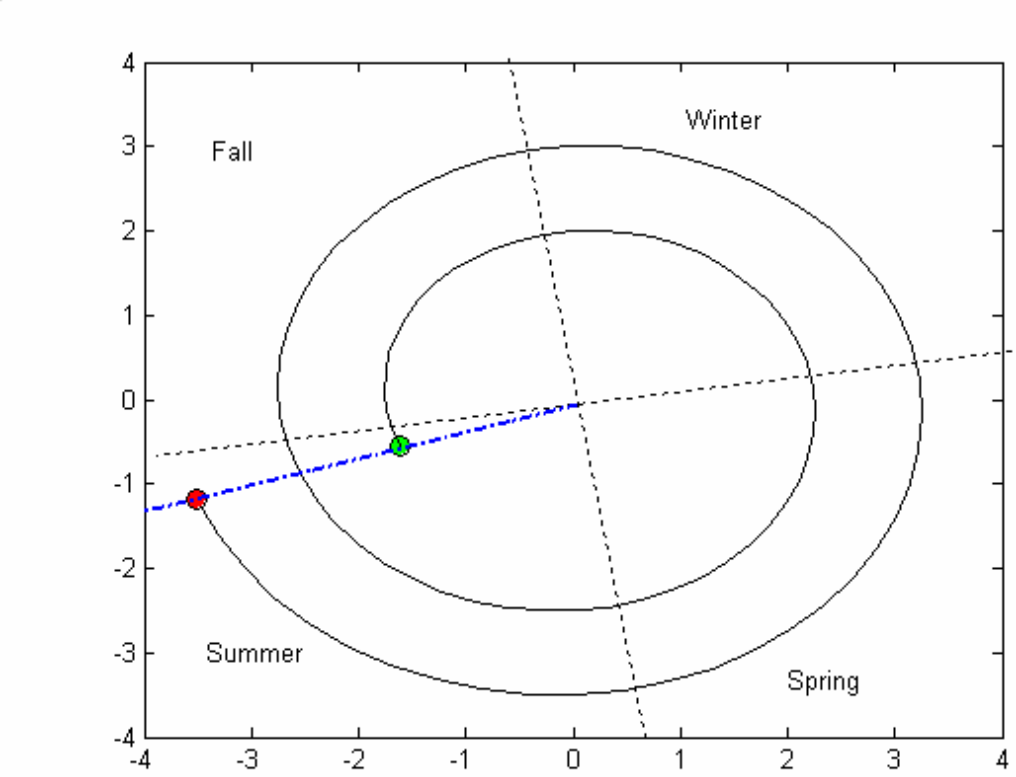


**Figure 9.** Winding graph (nondimensional axes) of *G*-function iterates for the 1995 Railroad Ridge temperature series, where the scaled polar transformed starting ovipositional date (innermost circle) is plotted against the ending scaled polar-transformed median adult emergence date (red). The transformed date is scaled such that JD 1 translates to the (*x,y*) coordinates (0,1), JD 365 translates to (0,2), and so on. The winding number is (number of fixed points plotted –1)/(number of years). Fixed points attracting populations to oviposition at the same time of year (synchronous emergence) will result in points aligning on the radial vector (dash-dot line). Dotted lines correspond to solstices and equinoxes to indicate time of year.

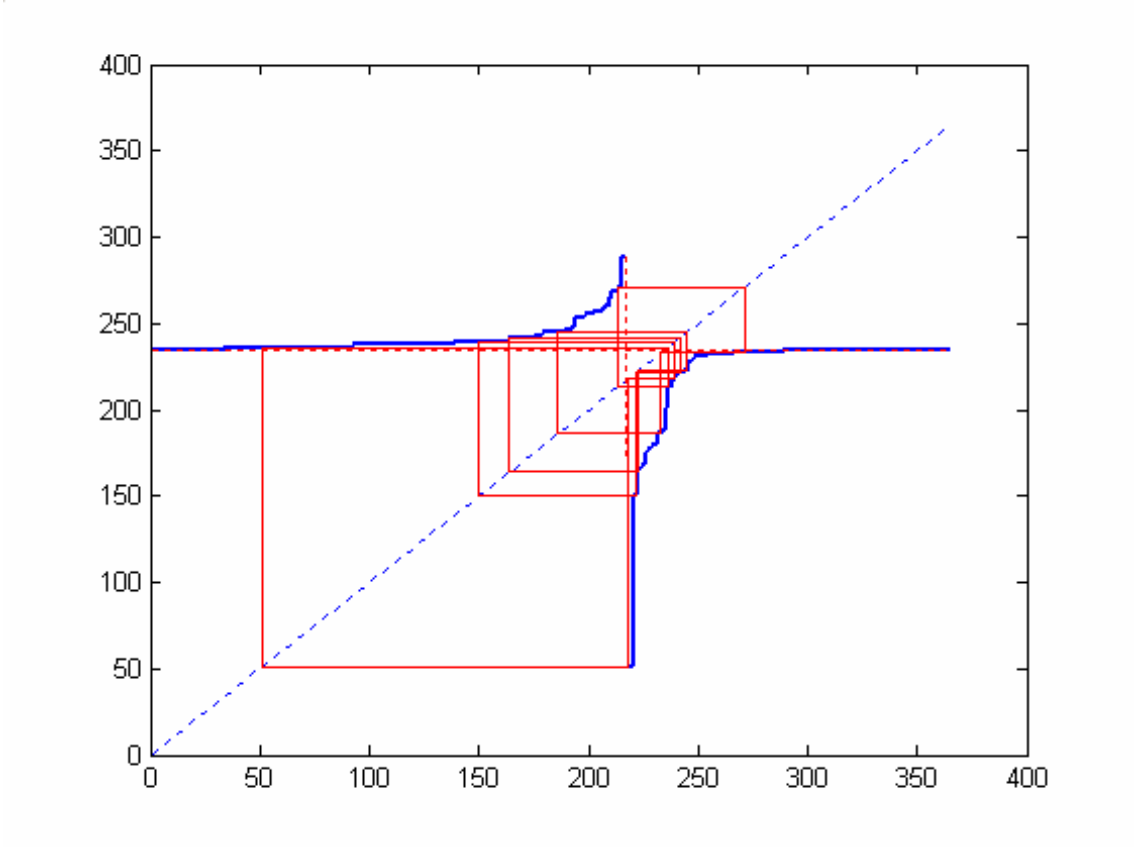


**Figure 10.** *G*-function generated by adding one centigrade degree to observed phloem temperatures for Railroad Ridge, 1995. Horizontal axis is input oviposition date for the *n*th generation and the vertical axis is median ovipositional date for the *(n+1)*st generation (reduced modulo 365). Intersections with the dotted 1-1 fixed point line (dashed) denote fixed points, which do not exist for this temperature series, indicating asynchrony. Cobwebbed iterates of the map, corresponding to a complicated 23/16 orbit are indicated in red.

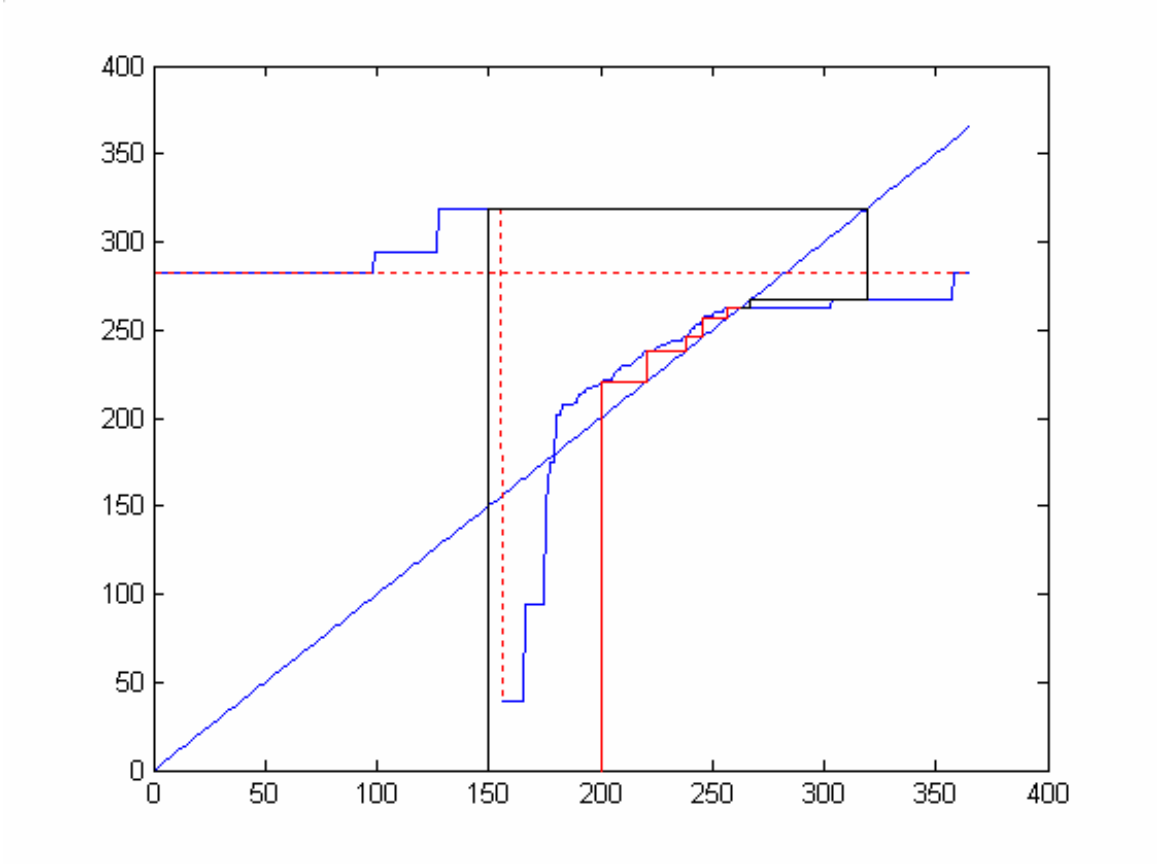


**Figure 11.** *G*-function generated by adding three degrees centigrade to phloem temperatures for Railroad Ridge, 1995. Horizontal axis is input oviposition date for the *n*th generation and the vertical axis is median ovipositional date for the *(n+1)*st generation (reduced modulo 365). Intersections with the dotted 1-1 fixed point line (dashed) indicate fixed points. In this case the stable fixed point occurs around JD 250, in early September. Cobwebbed iterates from an initial oviposition date of 200 are indicated in red.

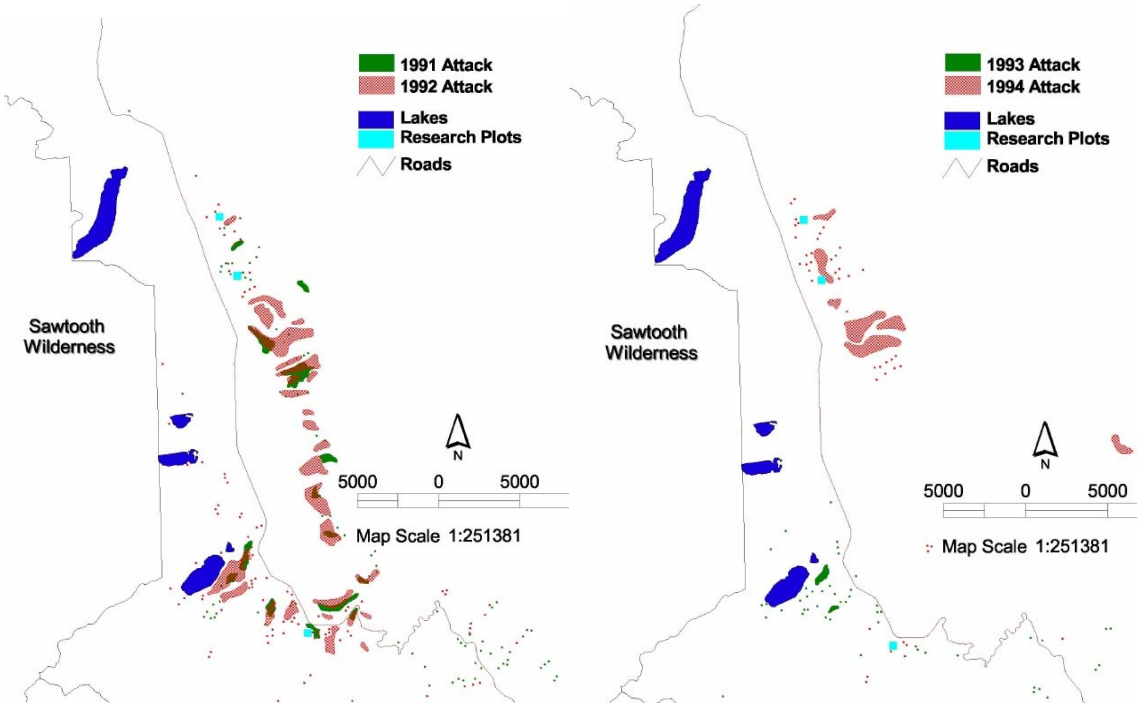


(a) (b)

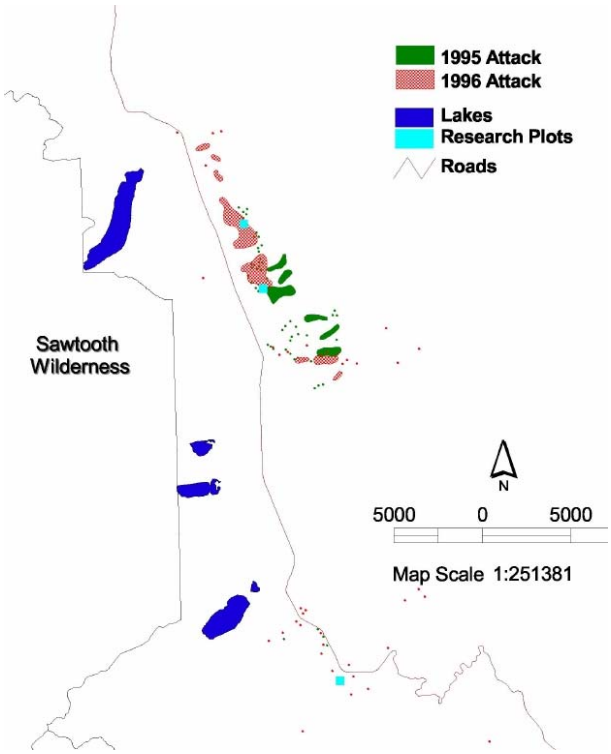


**Figure 12.** Six years of mountain pine beetle attacks in the Stanley Valley of Idaho, adjacent to the Sawtooth National Recreation Area. The sequences of attacks indicate the effect of the Pinatubo eruption (1993 had the coolest summer temperatures on record for the twentieth century in the Stanley basin. Each of the maps contains two years of forest polygons collected by the Aerial Damage Survey of the USDA Forest Service. In each map, the upper lake is Redfish Lake and the lower lake is Alturas lake; the grey line to the right of the lakes is Idaho highway 75 and the grey line to the left of the lakes is the boundary of the Sawtooth National Recreation Area. Maps are scaled in meters.

In (a) the sequence of yearly attacks for (green) and 92 (red cross hatch) are shown, indicating a relatively uniform progression of infestation. Mount Pinatubo erupted in 1992, lowering temperatures in the valley by several degrees during the summer of 1993. The effects of this temperature decline are illustrated in map (b), where 93 attacks appear in green and 94 in red cross hatch. The area with successful attack is at a decadal low during 1993, indicated by the small amount of green in (b). When temperatures rebounded in subsequent years, bark beetle attacks got back on track, and have been on a growing curve since that time, as indicated by the steadily increasing area attacked in 1995 (green) and 1996 (red cross hatch).

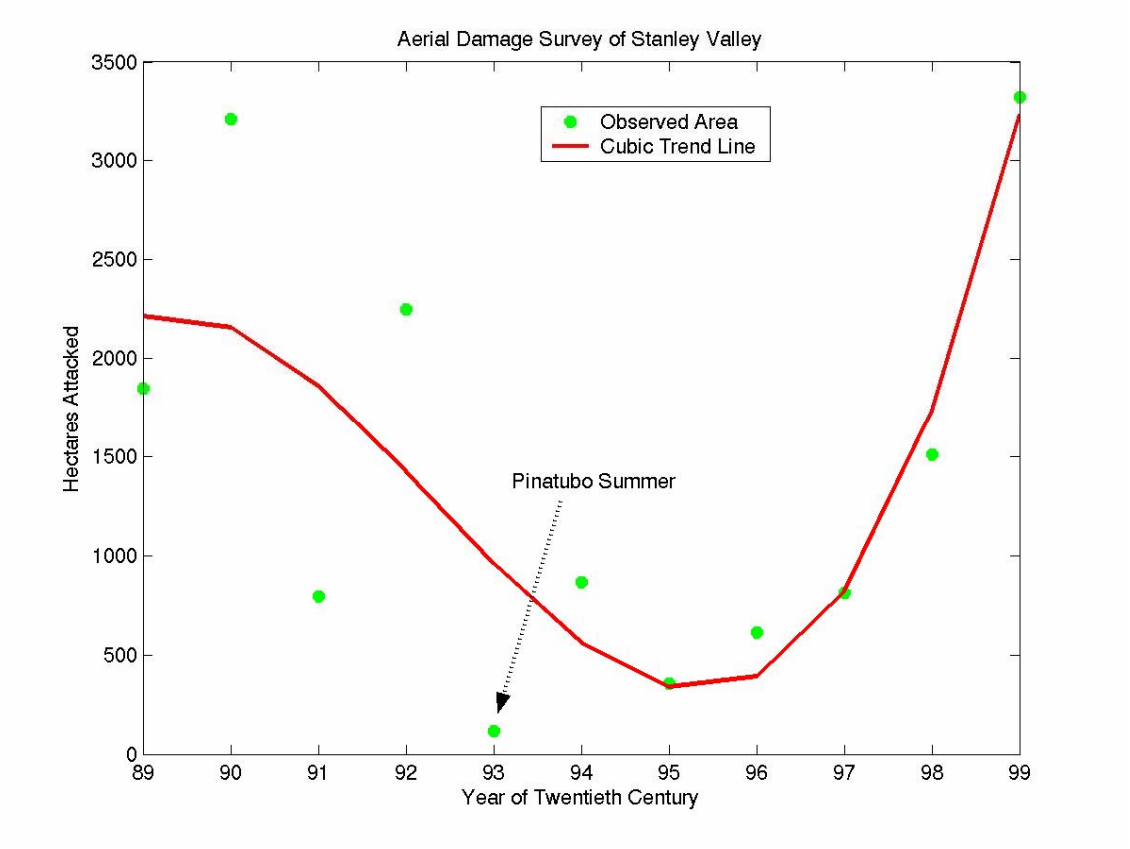


**Figure 13.** Total forest area in Stanley Basin impacted by mountain pine beetle from 1990-2000, generated by total area enclosed by polygons in ADS overflight data. Actual data points are plotted as circles; the solid curve is a cubic trend curve fitted to the data. The 1993 Pinatubo summer generates a clear minimum of impacted area; subsequent, warmer years have put the population back on a clear growth curve, which has continued on to epidemic levels by summer of 2002.

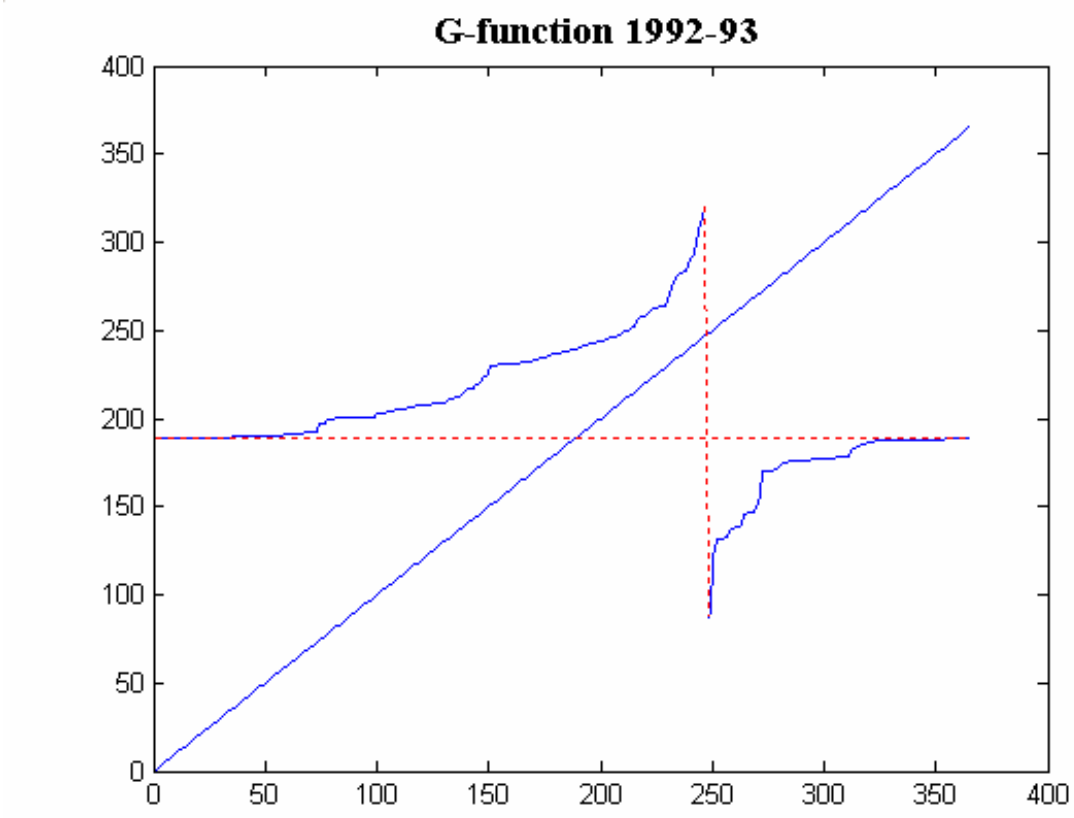


**Figure 14**. *G*-function plot generated by 1992-93 temperatures in the Stanley Basin, during the Pinatubo Perturbation. Julian days of oviposition in generation *n* and *n+1* are plotted on horizontal and vertical axes, respectively. Record low summer temperatures result in the nonexistence of univoltine fixed points and very late oviposition dates, making the these temperatures maladaptive for mountain pine beetles. As a consequence, attacks on lodgepole pine were strongly suppressed during the summer of 1993.

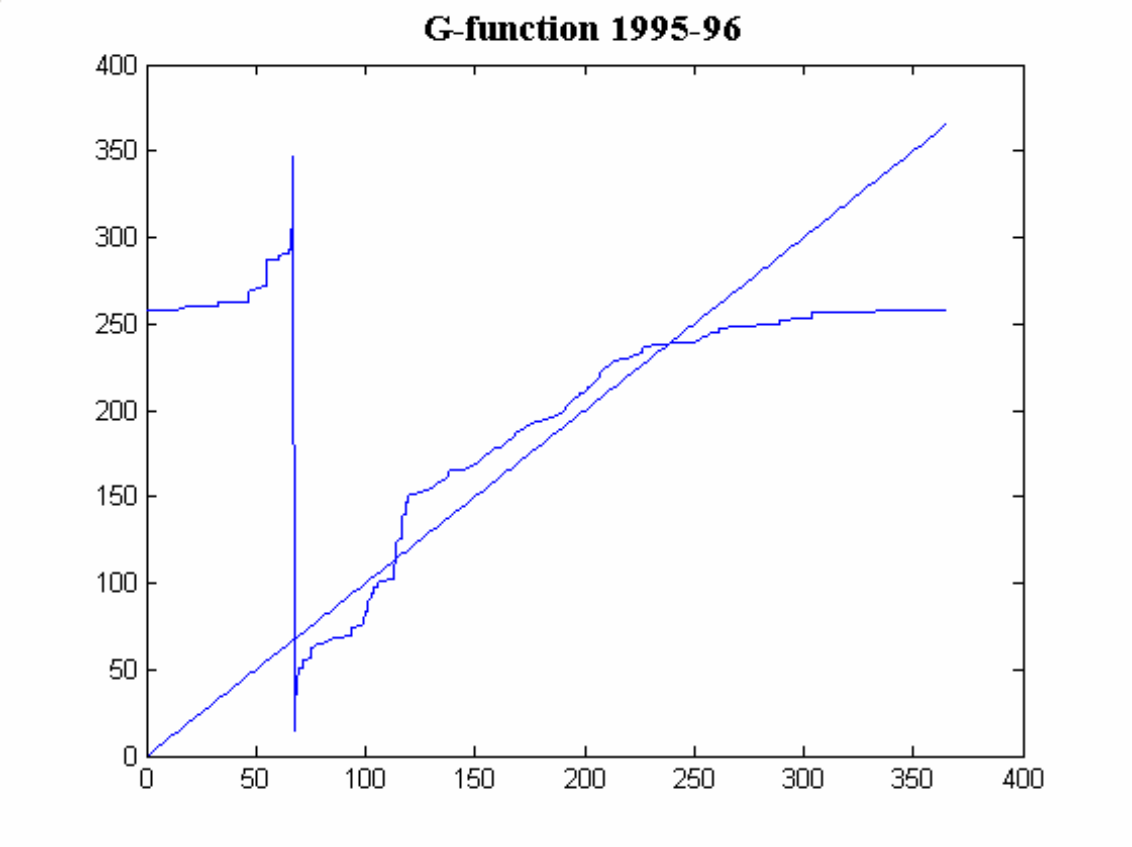


**Figure 15**. *G*-function generated by the more normal 1994-95 temperatures in the Stanley Basin. Julian days of oviposition in generation *n* and *n+1* are plotted on horizontal and vertical axes, respectively. Warmer summer temperatures result in a stable fixed point for oviposition dates at a reasonable time of year (JD 230, mid-August), indicating an adaptive seasonality. This and continued warm temperatures for the last several years have generated a population outbreak in the Basin.

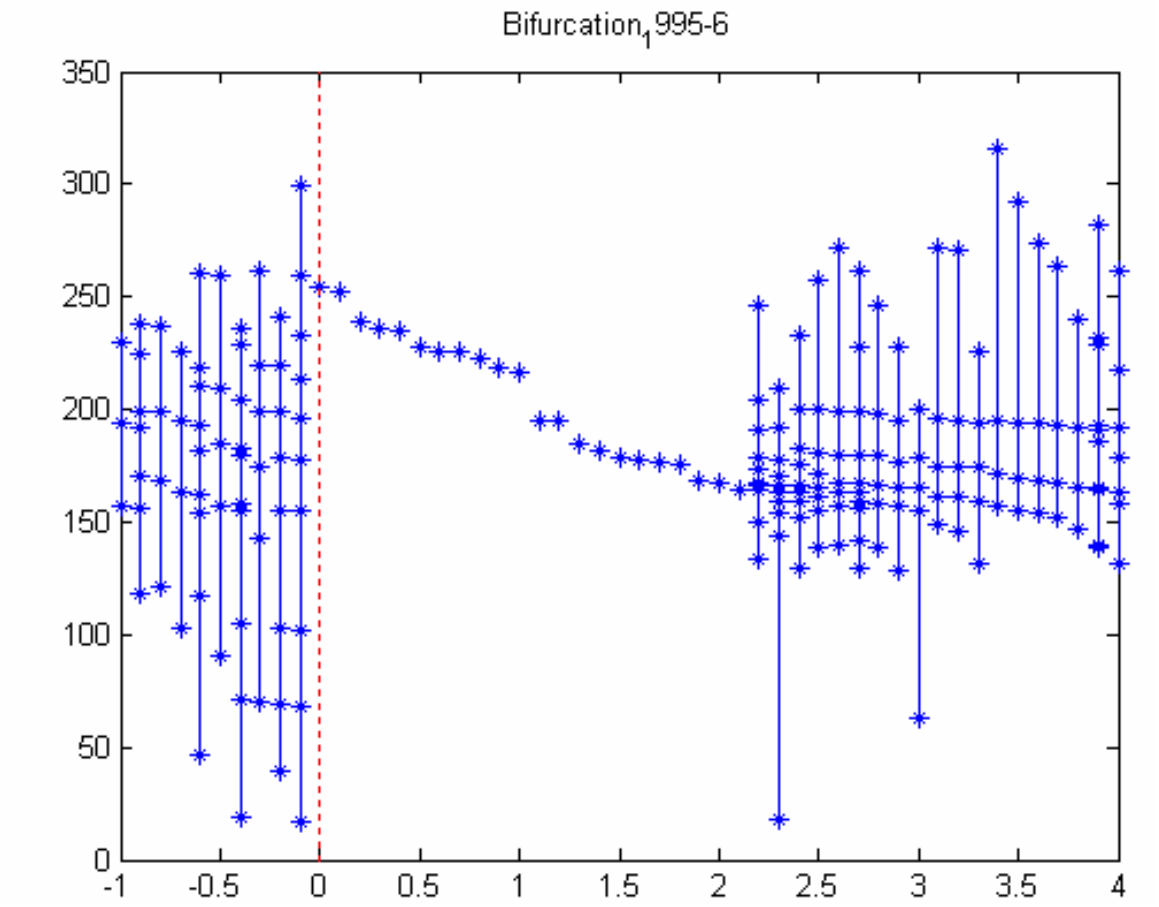


**Figure 16**. Bifurcation plot of *G*-function iterates relative to the 1995 Stanley Basin temperature series. Amount of mean temperature added to every element of temperature series appears on horizonatal axis in Centigrade degrees (so that 0 is the unperturbed 1995 temperature series); the last several iterates of the *G*-function are plotted on the vertical axis in Julian days. Unperturbed temperatures are at the beginning of a broad band of univoltine temperatures, indicating that continued warming should result in expanding growth of MPB populations.

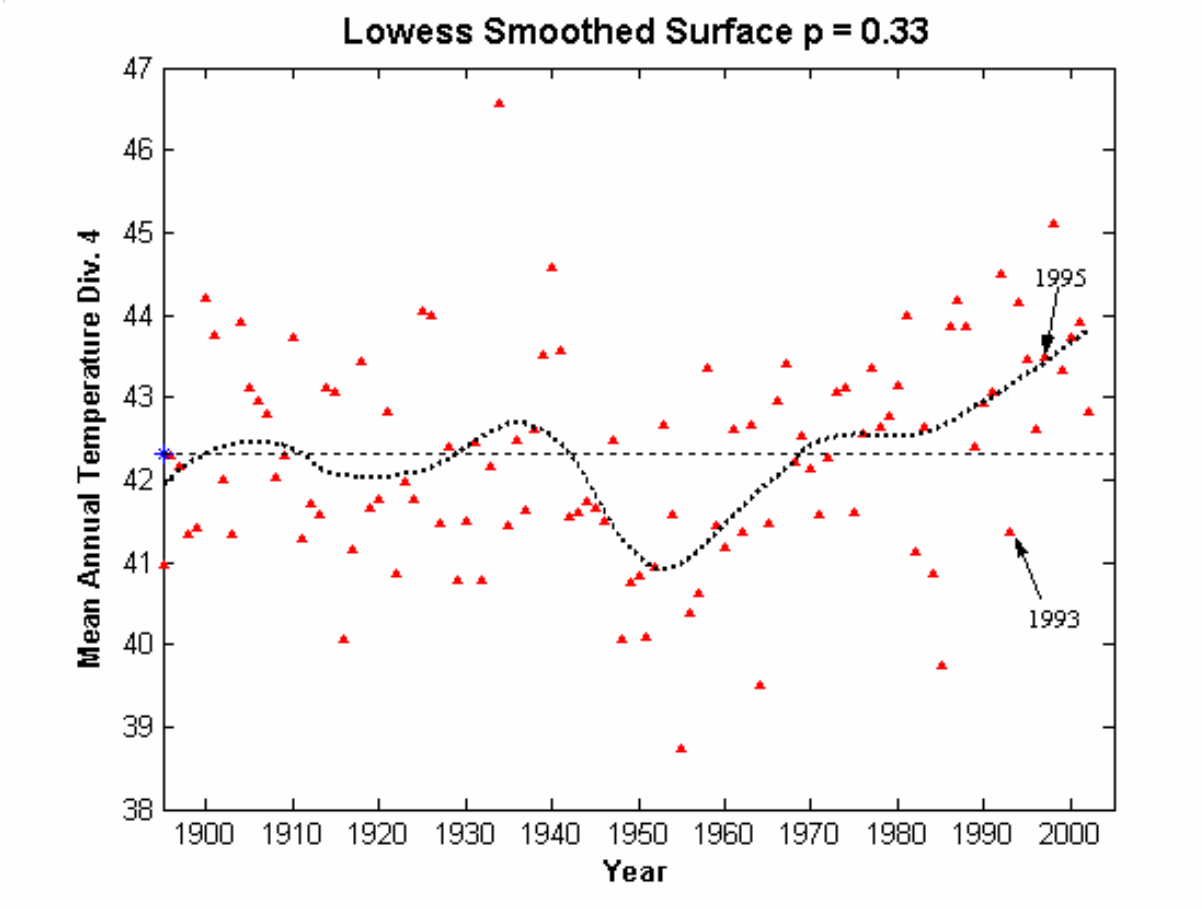


**Figure 17.** Annual mean temperatures for NCDC Division 4, including the Stanley Basin, smoothed by a Robust Lowess Quadratic fit that includes a bracket of 1/3 of the data for each estimated smoothed point Note the strong increasing trend from 1980 on and the relative position of the 1993 and 1995 years, well below and at the trend line, respectively.